DENDRON STABILIZED HYBRID NANOPARTICLES: SYNTHESIS, CHARACTERIZATION, AND ENERGY TRANSFER STUDIES

A Thesis

Presented to

the Faculty of the Department of Chemistry

University of Houston

In Partial Fulfillment

of the Requirements for the Degree

Master of Science

By

Katherine M. Puno

August 2012

DENDRON STABILIZED HYBRID NANOPARTICLES: SYNTHESIS, CHARACTERIZATION, AND ENERGY TRANSFER STUDIES

_____

Katherine M. Puno

APPROVED:

_____

Dr. T. Randall Lee, Chairman

_____

Dr. Rigoberto C. Advincula

_____

Dr. Randolph P. Thummel

_____

Dr. Roman S. Czernuszewicz

_____

Dr. Deborah Frigi Rodrigues

_____

Dr. Mark A. Smith,

Dean, College of Natural Sciences and Mathematics

ACKNOWLEDGMENTS

I have met a lot of people in my graduate school journey. Each one is worth noting for a lesson or two learned. It has been quite an adventure that I will always be thankful for.

I am especially, gratefully indebted first and foremost to Dr. Rigoberto Advincula, my research advisor who has given me the opportunity to work and learn with his research group. His unselfish support and professional guidance both in academics and life in general will always be treasured. As my mentor he has taught me not only scientific research but the importance of prioritizing the people and things that matter most in life.

To my committee members, Dr. Randall Lee, Dr. Randolph Thummel, Dr. Roman Czernuszewicz, and Dr. Deborah Rodrigues for their criticism, patience, and understanding.

To the members of the Advincula group past and present, thank you so much for the support, guidance, and friendship: Jane, Cel, Nicel, Roderick, Ed, Ajay, Deepali, Subbu, Joey, Al, Kat, Kim, Brylee, Peng Fei, Allan, and Latesha.

To friends from other groups who generously gave their time and advice : Thanh, Gino, and Rio.

To Dr. Guloy, thank you. You have the kindest heart.

To Dr. Josh Hudson for training me to use the spectrofluorometer for fluorescence lifetime data. Thank you for your patience.

To Dr. Czader, Sean, John, Mau, Chich, Enrico, and Dindee who helped me in ways nobody else could. I will forever be grateful.

Most of all , I want to thank my mentor, Mary Jane Felipe, for all her guidance, patience, encouragement, and unselfish support up to the very end; nobody could ever equal what you have done for me in graduate school. Thank you for teaching me perseverance and perfection. Thank you for making it all possible.

Lastly, my years in graduate school would not have been bearable without the unconditional support from my Mom, Dad, and sister who have always pushed me to the finish line.

To my husband, Alex, who has always been a model of a great scientist for me and my kids, thank you for your love, patience, and support that you gave me all throughout. To my kids, Alexander and Nathan, for making me want to do more, for your future.

Above all, to the Lord whose ways are not always my way. Thank you for guiding me to the right path and decisions.

DENDRON STABILIZED HYBRID NANOPARTICLES: SYNTHESIS, CHARACTERIZATION, AND ENERGY TRANSFER STUDIES

An Abstract of a Thesis

Presented to

the Faculty of the Department of Chemistry

University of Houston

In Partial Fulfillment

of the Requirements for the Degree

Master of Science

By

Katherine M. Puno

August 2012

ABSTRACT

Hybrid organic-inorganic nanoparticles are developed as a new class of material with a wide range of application based on their spectroscopic and electrochemical properties. Designing these materials to fine tune their properties as an energy or charge transfer pair calls for an ease of synthesis to produce stable and tunable nanoparticles. Chapter 2 describes a facile synthesis of a nanoparticle-cored dendrimer with electroactive carbazole dendron conjugated onto the amine surface of a generation three cystamine-core PAMAM dendrimer. The disulfide on the cystamine core of this dendrimer is reduced to produce dendrons that stabilize the AuNPs. Such manner of synthesis avoids the tedious stepwise process of attaching the dendrons to the AuNPs by convergent approach. Spectroscopic and electrochemical properties of this system are reported. Chapter 3 discusses the energy transfer involved between CdSe quantum dots and Au nanoparticles placed proximal to each other. The CdSe quantum dots are stabilized by generational carbazole dendrons which provide a control in the distance of these nanoparticles thereby controlling the donor-acceptor interaction. Quite uniquely, the reduction of the Au^{3+} ions did not necessitate any external reducing agent. The formation of this hybrid nanoparticle is a one pot synthesis wherein the reduction of the Au^{3+} to Au (0) provides a simultaneous cross-linking of the carbazole units which overall affords the formation of a three-component hybrid nanoparticles. Generally there is a potential in exploring the optimization of this facile synthetic protocol to produce the customized hybrid nanoparticles needed for specific optoelectronic applications.

TABLE OF CONTENTS

LIST OF FIGURES

LIST OF SCHEMES

LIST OF TABLES

ABBREVIATIONS

AuNPs	Gold Nanoparticles
CBzBr	Bromocarbazole
CdSe	Cadmium Selenide
CV	Cyclic Voltammetry
DCC	Dicyclohexylcarbodiimide
DEMNs	Dendrimer Encapsulated Metallic Nanoparticles
DENs	Dendrimer- Encapsulated Nanoparticles
DMAP	4-(Dimethylamino)pyridine
DMF	N,N-Dimethylformamide
DMSO	Dimethylsulfoxide
DSAuNPs	Dendron-stabilized Gold Nanoparticles
EDC	*N*-(3-Dimethylaminopropyl)-*N′*-ethylcarbodiimide hydrochloride
ET	Energy Transfer
FRET	Forster Resonance Energy Transfer
FT-IR	Fourier Transform Infrared
G1	Generation One
G1CBzBr	Generation 1 3,5-Bis(4-(9H-carbazol-9-yl)butoxy)benzyl Bromide
G1CBzCOOCH3	3,5-(Bis(4-(9H-carabazol-9-yl)butoxy)benzoate
G1CBzCOOH	3,5-(Bis(4-(9H-carabazol-9-yl)butoxy)benzoic acid

G1CBzOH	Genreration 1 3,5-Bis(4-(9H-carbazol-9-yl)butoxy)benzyl alcohol
G1CBzPE	Generation 1 3,5-Bis(4-(9H-carbazol-9-yl)butoxy)benzyl phosphonate ester
G1CBzPO	Generation 1 3,5-Bis(4-(9H-carbazol-9-yl)butoxy)benzyl phosphonic acid
G1CBzPO-CdSe	Generation 1 Phosphonic Acid Carbazole-Cadmium Selenide
G2	Generation Two
G2CBzCOOCH3	Generation 2 Methyl 3,5-Bis(3',5'-bis(4-(9H-carbazol-9-yl)butoxy)benzyloxy) Benzoate
G2CBzOH	Genreration 2 3,5-Bis(4-(9H-carbazol-9-yl)butoxy)benzyl alcohol
G2CBzPO-CdSe	Generation 2 Phosphonic Carbazole- Cadmium Selenide
G3	Generation 3
G3PAMAM-NHCOG1CBz	Generation 3 PAMAM Dendrimer with 3,5-(Bis(4-(9H-carabazol-9-yl)butoxy)amide
G4-OH	Generation Four Dendrimer with OH Functional Group
G4PAMAM	Generation 4 Polyamido Amine
GnCBzPO-Cdse-AuNP	Generation n Carbazole Phosphonic Acid Cadmium Selenide Gold Nanoparticle
$HAuCl_4$	Gold (III) Chloride Hydrate
HOMO	Highest Occupied Molecular Orbital
ITO	Indium Titanium Oxide

LUMO	Lowest Unoccupied Molecular Orbital
MUA	11-Mercaptoundecanoic Acid
$NaBH_4$	Sodium Borohydride
NBS	N-Bromosuccinimide
NCDs	Nanoparticle-Cored Dendrimers
NSET	Nanoparticle Surface Energy Transfer
OLEDs	Organic Light-Emitting Diodes
P3HT	3- Hexylthiophene
P3T	Terthiophene Dendron
P7T	Heptathiophene Dendron
PAMAM	Poly-amido Amine
PC	π-Conjugated Carbazole
$PdCl_4$	Palladium Tetrachloride
PEDOT:PSS	Poly(3,4-ethylenedioxythiophene)poly(styrenesulfonate)
PT	π-Conjugated Terthiophene
QD	Quantum Dots
ROMP	Ring Opening Metathesis Polymerization
SPR	Surface Plasmon Resonance
TBAH	Tetrabutyl Ammonium Hexafluorophosphate
TEM	Transmission Electron Microscopy
THF	Tetrahydrofuran
TLC	Thin-Layer Chromatography

TOAB	Tetraoctyl Ammonium Bromide
TOPO	Trioctyl Phosphonic Oxide
XPS	X-ray Photoelectron Spectroscopy
τ_d	Lifetime of Donor without Acceptor
τ_{da}	Lifetime of Donor with Acceptor

Chapter 1. Introduction

1.1. Hybrid Organic-Inorganic Nanoparticles

A hybrid material is a product of the physical or chemical combination of two or more different components, usually organic and inorganic, to produce a new composite with superior properties compared to the original individual components. Such materials have gained great interest in the field of materials research especially with the advent of facile and reproducible nanoparticle synthesis in the past decade.[1] Interestingly, organic π-conjugated polymers have been combined with metallic or semiconducting nanoparticles or nanocrystals as stabilizing ligands to afford a more stable, processable, soluble, rigid nanoparticles to enhance their optoelectronic properties by means of energy or charge transfer. [2]

The pioneering work of Alivisatos, combined the hole-accepting property of a conjugated polymer, 3-hexylthiophene (P3HT), with the electron-accepting property of semiconducting nanocrystals, CdSe, to fabricate materials for organic solar cells.[3] Although limited by high cost, for many years, inorganic solar cells have shown superior performance, with efficiency of 15-30%, over organic solar cells mainly because inorganic semiconductors have higher intrinsic carrier mobility, i.e. charges are more efficiently brought to the electrodes thereby reducing current losses.[4] Conjugated polymers on the other hand have very low carrier mobility due to the presence of electron traps like oxygen.[5] Combining the properties of inorganic semiconductors with the hole-accepting properties of conjugated polymers can open a wide area of research for more

efficient, yet cheaper, organic solar cells. In this work, the hybrid material of CdSe-P3HT, outperformed the inorganic semiconducting solar cells by producing a power conversion efficiency of up to 55%.[3]

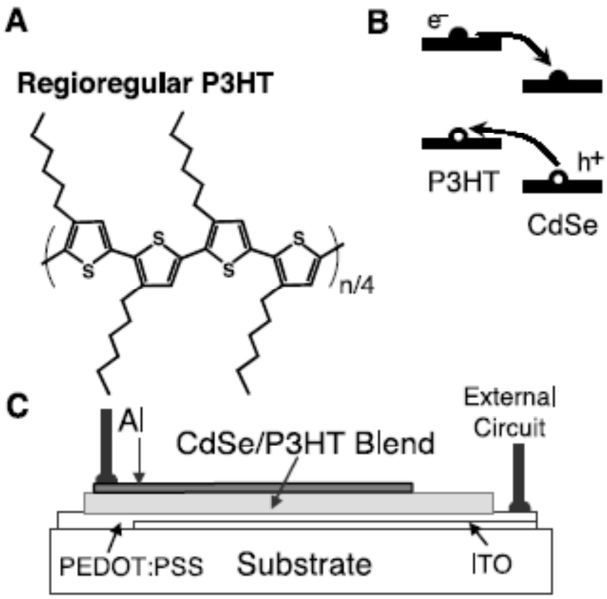

Figure 1.1 (a) structure of P3HT (b) energy level diagram of charge transfer (c) device structure of the film between Al electrode and PEDOT:PSS (Adapted with permission from ref 3. Copyright 2002 Science.)

Hybrid nanocomposites consisting of semiconducting quantum dots and conjugated polymers have in recent years attracted much attention for their use in both light emitting displays and photovoltaics, [6] primarily because of the spectral tunability and photostability of the quantum dots.

1.1.1 Dendrimer Encapsulated Nanoparticles

Another type of hybrid nanocomposite was pioneered by the group of Crooks. These are the dendrimer-encapsulated nanoparticles, or DENs where the metal ions are initially complexed into the interior of a dendrimer and then reducing the ions to form zero-valent DENs as shown in Figure 1.2.[7] The dendrimer serves as a template to immobilize the complexed ions and as dendron boxes to support the *in situ*-reduced metallic nanoparticles. More importantly, the dendrimers add an advantage to the properties of the nanoparticles in that they can prevent aggregation, keep them close to monodispersed size, control their solubility and processablity, and control their surface chemistry by manipulating the terminal group of the dendrimers. [8] These metal nanoparticles with dimension of < 4nm, formed within the dendrimers have interesting optical, electrical, and magnetic properties finding their way in practical applications such as catalysis, biosensors, and optoelectronic devices.[9]

1.1.2. Nanoparticle-cored Dendrimers

Nanoparticle-cored dendrimers (NCDs) are another class of hybrid nanomaterials that are metal containing dendrimers led by the group of Fox.[10] These dendrimers have gold nanoparticles in the core, stabilized by Frechet-type dendron wedges with disulfide functionality that self-assemble on the surface of the gold nanoparticles (AuNPs). The synthesis of this NCDs follow a modified procedure of the Brust method where in $HAuCl_4$ is reduced by the addition of $NaBH_4$ to produce AuNPs and subsequently

stabilized by thiolated dendrons. These dendrons are attached radially onto the central nanoparticles via Au-S bonds. The same process was done by the group in preparing palladium nanoparticles stabilized by large dendron wedges by reducing $PdCl_4$ with $NaBH_4$ in toluene in the presence of tetraoctyl ammonium bromide (TOAB) as phase transfer agent.[11] The general advantage of preparing nanoparticles in the center of a dendrimer for catalytic functions lies in the fact that the larger the dendrons used, the less dendrons actually attach on the surface of the metallic nanoparticle due to steric hindrance. This design gives a larger surface area of the core metal to act as a catalyst and not be completely hindered by the dendrimer as may be possible with DENs.[11]

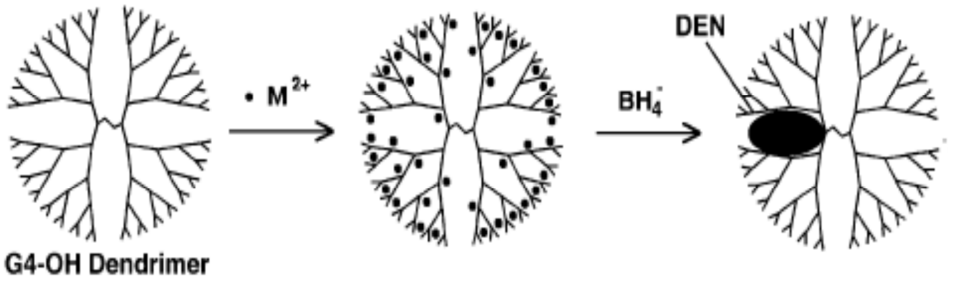

Figure 1.2 General scheme of the formation of dendrimer encapsulated nanoparticles (DENs) (Adapted with permission from ref 7. Copyright 2005 American Chemical Society)

1.2. Dendrons and Dendrimers

Dendrimers are monodisperse macromolecular architectures possessing a unique and well-defined structure containing connectors and building blocks arranged around a core.[12] This highly symmetric hyperbranched macromolecule consists of three main components: the core, the layers of branched repeat units connected to the core, and the

end groups at the periphery of the structure. Considered as a subclass of dendrimers, the wedge-shaped individual branching structures are called the dendrons. The ability to tailor the three parts of the dendrimer has led to platforms for study in the field of hybrid organic-inorganic materials. Fine-tuning the dendron and dendrimer's generational size and peripheral group density has permitted unprecedented control of the cavity size, shell structure and even shielding of the core from the surrounding environment.[13]

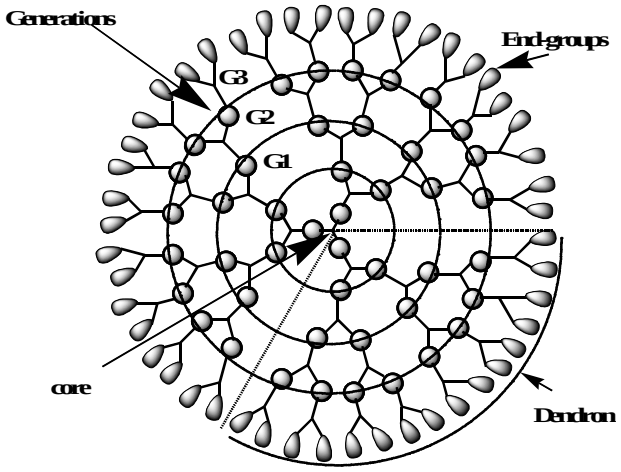

Figure 1.3. Typical dendrimeric structure composed of the branching units called the dendrons, the generations (G1, G2, G3), and the core molecule.

1.2.1. Synthesis of Dendrimer

Dendrimers are usually synthesized either via a convergent, divergent, or combined convergent/divergent approaches.[14] In the divergent approach, dendrimers are synthesized in a stepwise manner starting from the reactive core and continues outward by the repetition of coupling and activation steps (Figure 1.3). This method has successfully been used to synthesize high generation poly(amido amine) (PAMAM) and

poly(propylene imine) (PPI) dendrimers,[15] triazine dendrimers,[16] and Click-constructed dendrimers.[17]

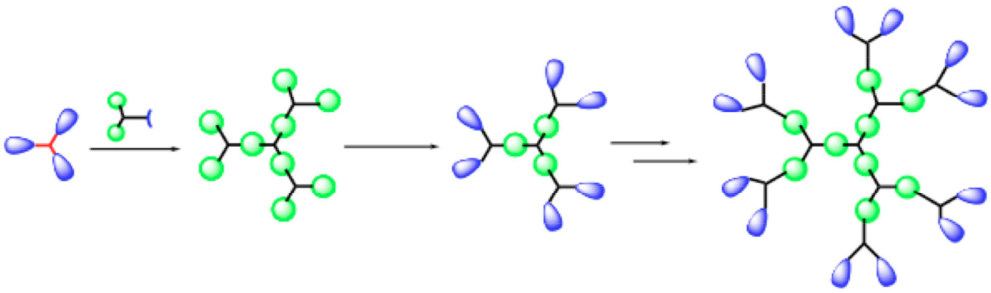

Figure 1.4. Divergent approach in synthesizing dendrimers starting from the core to the periphery.

Another method for constructing dendrimers involves the preparation from the periphery or surface towards the core. In this convergent approach (Figure 1.5), "one to one" coupling of the monomers is done initially to produce the dendrons which are then joined together with the core to create the dendrimer. Dendrimers synthesized via this method include Frechet-type poly(aryl ether) dendrimer,[18] Yamamoto carbazole dendrimer,[19] Mullen-type conjugated dendrimer,[20] and Astruc's giant redox metallodendrimer.[21] Our group has also successfully synthesized conjugated Frechet-type carbazole,[22] thiophene,[23] and terthiophene[24] dendrons and dendrimers through a convergent approach even employing a sonication method.

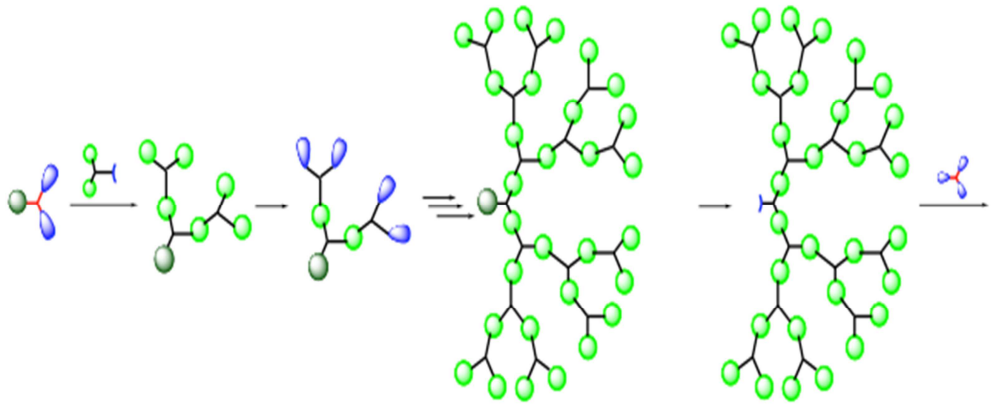

Figure 1.5. Convergent approach in synthesizing dendrimers starting from the periphery to the core.

1.2.2. Dendrons as Ligands in Nanoparticle Synthesis

Previous studies have shown that dendritic ligands can stabilize nanoparticles producing interesting hybrid inorganic-organic nanomaterials.[25] Fox *et al.* demonstrated that as the surface groups of the dendritic ligand become close-packed at the periphery of the hybrid material, these ligands offer a relatively low degree of surface passivation even at low loadings of the ligand onto the metal surface.[10] Several groups illustrated that cross-linking the dendritic shell around the Au nanoparticles imparts further stability to the hybrid nanomaterial through conversion of the monodentate ligand to a polydentate

network.[26] Using ring-opening metathesis polymerization (ROMP), Chechik *et al.* reported the synthesis of a thermally-stable Au nanoparticle via cross-linking of norbornene dendron ligands.[27] This same group has further extended their work into using alkenyl-terminated dendritic ligands and successfully intra-molecularly cross-linked them using Grubbs second generation catalyst which has resulted to nanoparticles having enhanced kinetic stability as demonstrated by cyanide etching and thermal ripening.[27]

Conducting polymers and dendrimers have been extensively studied and used as stabilizing agents to form metallic and semiconducting nanocrystals.[28.29] Conducting polymers are conjugated polymers that owe its conducting property based upon its conjugated structure or the pi molecular orbitals delocalized along the polymer chains. Because they are polymeric in structure, they form a more robust structure and have better processability than their non-polymeric counterpart. [30] Among the more prominent conjugated polymers that have been extensively studied for their effective conductivity are polyanilines, polypyrroles, and polyacetylenes while those that are studied for their photoluminescent properties include polythiophenes, polyphenylenes, polyfluorenes, poly-(arylenevinylene)s, and poly(phenyleneethynylene)s.[28]

Conjugated conducting polymers and dendrimers have gained great interest in the field of hybrid organic/inorganic nanoparticles because their unique properties and flexible synthesis makes them suitable encapsulating stabilizing ligands in the formation of nanoparticles. [29] Not only do they prevent aggregation of the metallic or semiconducting nanoparticles, they also fine tune the processability and solubility of the

nanoparticles based on the peripheral functional groups present in the structures of these organic ligands. In addition, the presence of conjugated ligands can also facilitate intermolecular energy or charge transfer from the pi conjugation to the central nanoparticles thus making them useful for optoelectronic and biosensing applications.[28,29]

1.3. Photoluminescent Quantum Dots

Quantum dots are highly luminescent semiconductor nanocrystals with sizes in the 1–10 nm range. At this dimension, the optical properties of the nanocrystals significantly differ from that of their bulk counterpart due to quantum confinement.[31] The smaller the nanocrystal is, the larger is the band gap between its conduction and valence bands, allowing for wider absorption wavelengths and narrow tunable emission wavelength. Controlling the size and even the shape of these quantum dots tunes their optoelectronic properties. Because of their bright emission, quantum dots have been used in many studies for application as organic light emitting diodes (OLEDS), [32] photovoltaic and solar cells. [33]

Several known stabilizing ligands or surfactants have been used when synthesizing quantum dots to prevent aggregation. [34] These ligands are needed to control the monodispersity of the size of the quantum dots as well as their solubility and functionalization. This can be achieved by either direct synthesis onto the growing nanocrystal or by ligand exchange with another surfactant that has a strong affinity to the quantum dots. Among these ligands are those with phosphonic acid, carboxylic acid, and

amine moeities.[35] In most cases, these ligands are purely organic, the most common one of which is the trioctyl phosphonic oxide (TOPO).

Conjugated organic polymers or dendrons that are used as stabilizers for quantum dots serves also to improve the electron or hole injection process onto the CdSe to realize energy or charge transfer as in the case of the work of Skaff *et al.* [36a] wherein they used poly- (*para*-phenylene vinylene) wherein they used phosphine oxide group at the end of the polymer to produce an OLED using light emitting quantum dots. On the other hand, the group of Wolf [36b] as well as the group of Advincula[37] used oligothiophene anchored onto the CdSe to facilitate electron transfer from the high-energy highest occupied molecular orbital (HOMO) of the longer chain oligothiophene to the CdSe quantum dots effecting a quenching of the latter's fluorescence. Such phenomenon is useful in the fabrication of photovoltaic films.

1.4. Plasmonic Gold Nanoparticles

Gold nanoparticles (AuNPs) possess special chemical and physical properties that make them ideal materials for fabrication of chemical and biological sensors and catalysts. [38] In the nanometer regime, AuNPs exhibit quantum size effects that allows them to have discrete electron transition energy levels thus they can have different oxidation states. [39] Moreover, when a photon hits the surface of the AuNP, the electrons on the surface of the metal produce an oscillation with nanometer-size wavelength in resonance with the wavelength of the incident light. [40] This collective oscillation of the

conduction electron is called surface plasmon resonance (SPR) as depicted in Fig. 1.6. which can pick up light and carry it along the metal surface because of resonant excitation by the photon.[41,42] These plasmons can focus light into very tiny spots, and even direct light in complex circuits in nanometer scale which far exceeds the resolution limits of conventional optics. [41] By altering the structure, shape or size, of the metal, its surface plasmon properties can be tailored as well.[40] Thus in the field of photonics, surface plasmons are one of the most studied systems from optoelectronic devices to cancer research.

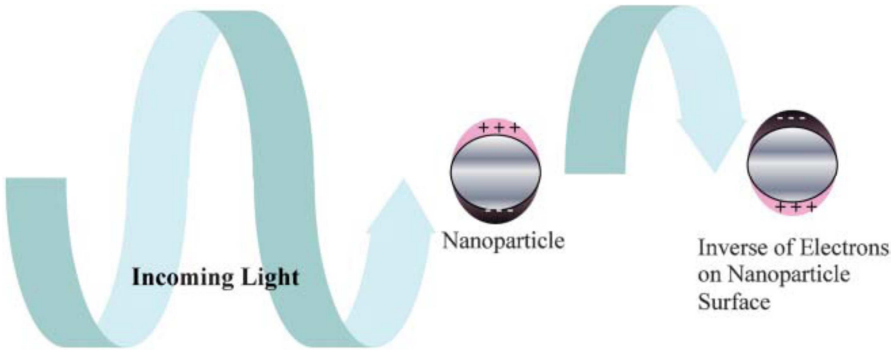

Figure 1.6. Surface Plasmon Resonance due to interaction of conduction band electron with incident light. Adapted with permission from ref 42. Copyright 2012 American Chemical Society.

Another important characteristic of AuNPs is that they serve as efficient fluorescent quencher in many Forster Resonance Energy Transfer (FRET) -based assay. [43] This can be explained by AuNPs having high molar absorption coefficient and broad absorption energy spectra that is overlapped by the emission of chromophores or emission donors. [44] There have been many reported FRET- based biological assays [44], ion detections [45], and small organic molecule sensing. [46] AuNPs have also been coupled

with semiconducting quantum dots to exhibit energy transfer by quenching of the photoluminescence of the highly fluorescent quantum dots.[47]

The ease of synthesis of AuNPs adds to its attributes and in addition they are highly stable. The properties of these AuNPs are further customized by the ligands that stabilize them to control their solubility, size, shape, and functionality.[42] Brust and Schiffrin made the breakthrough in 1994 when they synthesized AuNP using two-phased synthetic method using the well-established thiol-gold interaction.[48] Following this synthetic method, several single-phase strategies followed suit to produce thiol-stabilized AuNPs.[49]

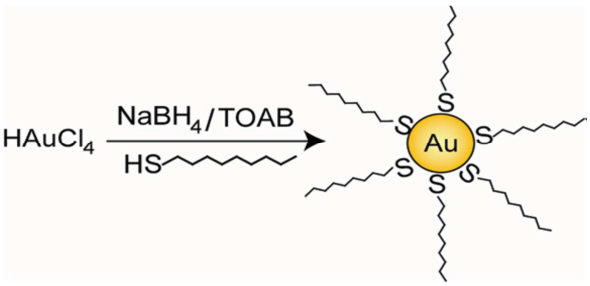

Figure 1.7. Brust-Schiffrin method of reducing gold and stabilizing with thiol ligands. Adapted with permission from ref 38. Copyright 2004 American Chemical Society.

1.5. Energy Transfer

One way to determine the relationship, and hence application, between the building blocks of a hybridized material is by understanding their coupling phenomena. One very common process that is studied in π-conjugated materials and nanoparticles is

their optical property using FRET wherein one component acts as a donor and the other is the acceptor. [50] FRET is defined as the non-radiative energy flow from an excited state donor exciton to the ground state of the acceptor through dipole-dipole interaction, considering the distance between the two components lie within the Forster radius which is less than 10nm. [51] Energy transfer (ET) studies enable understanding of the optical properties of these materials wherein ET is quantified by either quenching of the emission of the donor and the consequent increase in emission of the acceptor. [52] It can also be evidenced by the decrease in the excited state lifetime of the donor. [53]

Additionally the efficiency of the energy transfer can also be determined by fluorescence lifetime based on the following equation:

$$E = 1 - \frac{\tau_{DA}}{\tau_D}$$

where τ is the fluorescence lifetime. Again, the efficiency is higher if the fluorescence lifetime of the donor is sufficiently decreased in the presence of the acceptor which acts as the quencher.[54]

Our group has previously reported a study on the energy transfer involved in the interaction between electroactive π-conjugated oligothiophene [37] used as capping agent on CdSe quantum dots by ligand exchange synthesis. In this work they showed that oligomeric terthiophene can be used as stabilizing surfactants on CdSe nanocrystals using two varying sizes of these dendrons, one with three thiophene groups labled as P3T and another one with seven thiophene group labeled as P7T. Moreover this work investigated the feasibility of using this hybrid nanocomposite as a material for electron or hole

transporting device such as photovoltaic film. In both cases of varying oligothiophene sizes, the photoluminescence of the quantum dots and the dendrons were completely quenched which the group attributed to an electron or charge transfer occurring upon excitation of the nanocrystal. To test the effectiveness of the energy transfer, which in this case is direct photocurrent conversion, a simple photovoltaic device was fabricated by spin-casting P7T/nanocrystals onto clean Indium Titanium Oxide (ITO) substrate. The efficiency of the fabricated material was found on average to be 0.29%. Increasing the size and changing the shape of the nanocrystals is in principle believed to increase the efficiency of the device.

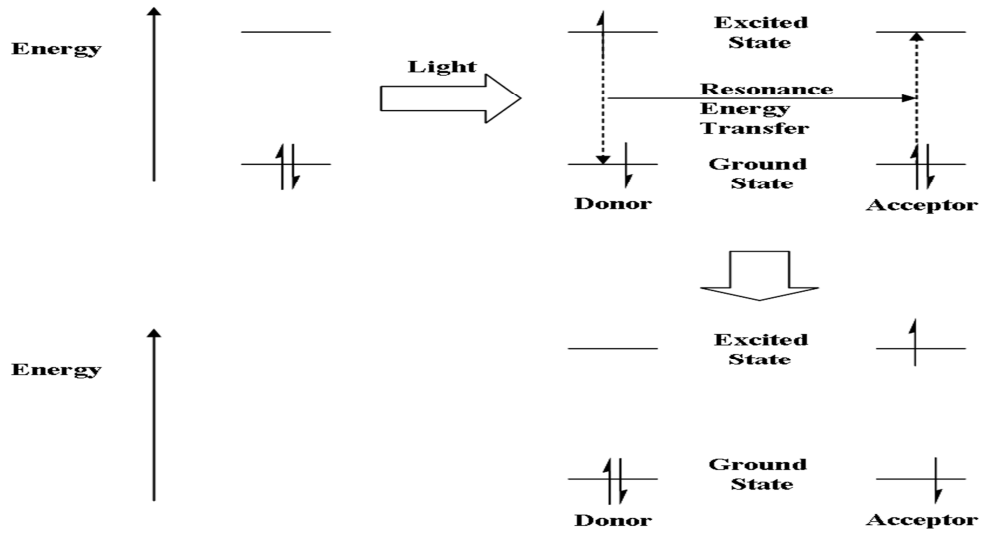

Figure. 1.8. Energy Transfer Diagram of photoexcited electron from donor to acceptor. Adapted with permission from ref 1a. Copyright 2011 American Chemical Society.

In another report by our group, a study on energy transfer was conducted on generation two of π-conjugated carbazole dendron which is Frechet-type polybenzyl ether with phosphonic acid moeity as stabilizing surfactant for CdSe quantum dots using a one-pot synthesis. [54] In this study, the absorbance and emission spectra showed an energy transfer occurred based on the overlapping of emission of the dendron on the absorbance of the CdSe nanoparticle. The electroactive π-conjugated carbazole dendrons acted as charge or electron donor and the CdSe nanoparticle acted as acceptor or as hole transport donor. Their overlapping spectra suggested their use for energy transfer or charge transfer application.

1.6. Objectives and Outline

The use of metal hybrid nanoparticles has been realized in the development of materials in various applications. A rational design of these materials involves the choice of ligand imparting stability and or control of its properties, the ease of synthesis, and exploring composites of different nanoparticles leading to the assembly providing excellent pairs in fine-tuning their optical properties.

The general objectives of this thesis are as follows: (1) to synthesize a hybrid organic-inorganic nanoparticle via one-pot direct synthesis methods providing a control of the size and interaction of these nanoparticles utilizing dendronic and dendrimeric architectures, and (2) to investigate the energy transfer mechanisms involved with

iteration of these materials in Au nanoparticles and CdSe nanocrystals by spectral analysis.

Chapter 2 details the facile synthesis of a nanoparticle-cored dendrimer with electroactive carbazole dendron from a generation three cystamine-core PAMAM dendrimer. The current study provides a simple strategy to fabricating a dendron-stabilized Au nanoparticle (DSAuNPs) avoiding the stepwise and time-consuming anchoring of dendrons produced via a convergent approach. In this work, we report the structural, spectroscopic and electrochemical properties of the easily-formed DSAuNPs, and the energy transfer involved between the gold nanoparticle and the carbazole dendron.

Chapter 3 investigates the energy transfer between QDs and Au nanoparticles in a single composite system providing a control in the distance of these nanoparticles via generational carbazole dendron ligands and thus, controlling their donor-acceptor interactions. Interestingly, the use of carbazole dendrons not only imparts the control of its proximal distance but also provides a unique composite system wherein no external reducing agent was needed to the reduction of Au^{3+} ions to Au^{0}. The system described herein is a direct synthesis method where the reduction of Au^{3+} to Au^{0}, simultaneously caused the cross-linking of the carbazole units enabling a three-component hybrid nanoparticle (GnCBzPO-CdSe-AuNP) system where n represents the generation of the ligand.

Finally, Chapter 4 provides a summary of the important findings on the design of metal-hybrid nanoparticles, how this affects the ease of its synthesis, and how imparting dendronic and electroactive materials affect its properties. A global conclusion is also given of the dissertation.

1.7. References

1. (a) Park, Y.; Advincula, R. C., *Chem. Mater.* **2011**, *23*, 4273. (b) Feldheim, D. L.; Grabar, K. C.; Natan, M. J.; Mallouk, T. E. *J. Am. Chem. Soc.* **1996**, *118*, 7640. (c) Beek, W. J. E.; Wienk, M. M.; Janssen, R. A. J. *Ad*v. *Mater.* **2004**, *16*, 1009.
2. (a) Lahav, M.; Weiss, E. A.; Xu, Q.B.; Whitesides, G. M. *Nano Lett.* **2006**, *6*, 2166. (b) Hu, J. T.; Ouyang, M.; Yang, P. D.; Lieber, C. M. *Nature* **1999**, *399*, 48. (c) Robel, I.; Bunker, B. A.; Kamat, P. V. *Ad*v. *Mater.* **2005**, *17*, 2458.
3. Huynh, W. U.; Dittmer, J. J.; Alivisatos, A. P. *Science* **2002**, *295*, 2425.
4. Liu, J.; Tanaka, T.; Sivula, K.; Alivisatos, A. P.; Frechet, J. M. J. *J. Am. Soc. Chem.* **2004**, *126*, 6550.
5. Bozano, L.; Carter, S. A.; Scott, J. C.; Malliaras, G. G.; Brock, P. J. *Appl. Phys. Lett.* **1999**, *74*, 1132.
6. (a) Chang, T. W.; Musikhin, S.; Bakueva, L.; Levina, L.; Hines, M. A.; Cyr, P. W.; Sargent, E. H. *Appl. Phys. Lett*. **2004**, *84*, 4295. (b) Huynh, W. U.; Peng, X. G.; Alivisatos, A. P. *Adv. Mater.* **1999**, *11*, 923. (c) Liu, J.; Tanaka, T.; Sivula, K.; Alivisatos, A. P.; Frechet,J. M. J. *J. Am. Chem. Soc*. **2004**, *126*, 6550. (d) Zorn, M.; Bae, W. K.; Kwak, J.; Lee, H.; Lee, C.; Zentel, R.; Char, K. *ACS Nano* **2009**, *3*, 1063.
7. (a) Scott, R. W. J.; Wilson, O.; Crooks, R. M. *J. Phys. Chem. B* **2005**, *109*, 692. (b) Scott, R. W. J.; Ye, H.; Henriquez, R. R.; Crooks, R. M. *Chem. Mater.* **2003**, *15*, 3873.

8. Knecht, M. R.; Garcia-Martinez, J. C.; Crooks, R. M. *Langmuir* **2005**, *21*, 11981. (b) Gomez, M. V.; Guerra, J.; Velders, A.H.; Crooks, R. M., *J. Am. Chem. Soc.* **2009**, *191*, 341. (c) Herrero, M. A.; Guerra, J.; Myers, V. S.; Gomez. M. V.; Crooks, R. M.; Prato. M. *ACS Nano* **2010**, *4*, 905.

9. Kim, Y. G.; Oh, S. K.; Crooks, R. M. *Chem. Mater.* **2004**, *16*, 167.

10. Godipas, K. R.; Whitesell, J. K.; Fox, M. A. *J. Am. Chem. Soc.* **2003**, *125*, 6491.

11. Godipas, K. R.; Whitesell, J. K.; Fox, M. A. *Nano. Lett.* **2003**, *12*, 1757.

12. (a) Grayson, S. M.; Frechet, J. M. *Chem. Rev.* **2001**, *101*, 3819. (b) Mintzer, M. A.; Grinstaff, M.W. *Chem. Soc. Rev.* **2011**, *40*, 173. (c) Friedhofen, J. H.; Vogtle, F. *New J. Chem.* **2006**, *30*, 32.

13. Christensen, J. B.; Boas, U.; Heegard, P. M. *J. Mater. Chem.* **2006**, *16*, 3785.

14. Tomalia, D. A. *Adv. Mater.* **1994**, *6*, 529.

15. van den Berg, E. M.; Meijer, D. *Angew. Chem.* **1993**, *105*, 1370.

16. Lim, J.; Mintzer, M. A.; Perez, L. M.; Simanek, E. E. *Org. Lett.* **2010**, *12*, 1148.

17. Joralemon, M. J.; O'Reilly, R. K.; Matson, J. B.; Nugent, A. K.; Hawker, C. J.; Wooley, K. L. *Macromolecules* **2005**, *38*, 5436.

18. Hawker, C.; Frechet, M. J. *J. Am. Chem. Soc.***1990**, *112*, 7638.

19. Higuchi, M.; Shiki, S.; Ariga, K.; Yamamoto, K. *J. Am. Chem. Soc.* **2001**, *123*, 4414.

20. Berresheim A.J.; Muller, M.; Mullen, K. *Chem. Rev.* **1999**, 99, 1747.

21. Ornelas, C.; Ruiz, J.; Astruc. D. *Organometallics* **2009**, *28*, 2716.

22. Taranekar, P.; Fulghum, T.; Patton, D.; Ponnapati, R.; Clyde, G.; Advincula, R. C. *J. Am. Chem. Soc.* **2007**, *129*, 12537.

23. Xia, C.; Fan, X.; Lockliin, J.; Advincula, R.C. *Org. Lett.* **2002**, *4*, 2067.

24. Ponnapati, R.; Felipe, M. J.; Park, J.; Vargas, J.; Advincula, R. C. *Macromolecules* **2010**, *43*, 10414.

25. Guo, W.Z.; Peng, X. G. *Comp. Rend. Chim.* **2003**, *6*, 989.

26. Koenig, S.; Chechik, V. *Langmuir* **2006**, *22*, 5168.

27. Love, C. S.; Ashworth, I.; Brennan, C.; Chechik, V.; Smith, D. K. *Langmuir* **2007**, *23*, 5787.

28. Pecher, J.; Mecking, S. *Chem. Rev.* **2010**, *110*, 6260.

29. Bronstein, L. M.; Shifrina, Z. C*hem. Rev.* **2011**, *111*, 5301.

30. Burroughes, J. H.; Bradley, D.C.; Brown, A. R.; Marks, R. N.; Mackay, K.; Friend, R.H.; Burns, P.L.; Holmes, A.B. *Nature* **1990**, *347*, 539.

31. (a) Hildebrandt, N. *ACS Nano* **2011**, *5*, 5268. (b) Murray, C. B.; Norris, D. J.; Bawendi, M. G. *J. Am. Chem. Soc.* **1993**, *115*, 8706. (c) Parak, W. J.; Gerion, D.; Pellegrino, T.; Zanchet, D.; Gupta, V. K. *Nanotech*. **2003**, *14*, 15. (d) Clapp, A. R.; Medintz, I. L.; Mauro, J. M.; Fisher, B. R.; Bawendi, M. G.; Mattoussi, H. *J. Am. Chem. Soc.* **2004**, *126*, 301.

32. (a) Guo, Z. S.; Zhao, L.; Pei, J.; Zhuo, Z. L.; Gibson, G.; Brug, J.; Lam. S.; Mao, S. S. *Macromolecules* **2010**, *43*, 1860. (b) Mitsuishi, M.; Morita, S.; Tawa, K.; Nishii, J.; Miyashita, T. *Langmuir* **2012**, *28*, 2313. (c) Munro, A. M.; Zacher, B.; Graham, A.; Armstrong, N. R. *ACS Appl. Mater. Interfaces* **2010**, *2*, 863.

33. (a) Kongkanand, A.; Tvrdy, K.; Takechi, K.; Kuno, M.; Kamat, P. V. *J. Am. Chem. Soc.* **2008**, *130*, 4007. (b) Kamat, P. V.; Tvrdy, K.; Baker, D. R.; Radich, J.

G. *Chem. Rev.* **2010**, *110*, 6664. (c) Buhbut, S.; Itzhakov, S.; Oron, D.; Zaban, A. *J. Phys. Chem. Lett.* **2011**, *2*, 1917.

34. Talapin, D. V.; Lee, J.; Kovalenko, M.; Shevchenko, E. *Chem. Rev.* **2010**, *110*, 389.

35. Burda, C.; Chen, X.; Narayanan, R.; El-Sayed, M. *Chem. Rev.* **2005**, *105*, 1025.

36. (a) Skaff, H.; Sill, K.; Emrick, T. J. *J. Am. Chem. Soc.* **2004**, *126*, 11322. (b) Sih, B. C.; Wolf, M. O. *J. Phys. Chem. C* **2007**, *111*, 17184.

37. Locklin, J.; Patton, D.; Deng, S. X.; Baba, A.; Millan, M.; Advincula, R. C. *Chem.Mater.* **2004**, *16*, 5187.

38. Daniel, M. C.; Astruc, D. *Chem. Rev.* **2004**, *104*, 293.

39. (a) Quinn, B. M.; Liljeroth, P.; Ruiz, V.; Laaksonen, T.; Kontturi, K. *J. Am. Chem. Soc.* **2003**, *125*, 6644. (b) Antonello, S.; Holm, A. H.; Instuli, E.; Maran, F. *J. Am. Chem. Soc.* **2007**, *129*, 9836.

40. Heber, J. *Nature* **2009**, *461*, 720.

41. Barnes, W. L.; Dereux, A.; Ebbesen, T. W. *Nature* **2003**, *424*, 824.

42. Saha, K.; Agasti, S. S.; Kim, C.; Li, X.; Rotello, V. M. *Chem. Rev.* **2012**, *112*, 2739.

43. Sapsford, K. E.; Berti, L.; Medintz, I. L. *Angew. Chem. Int. Ed.* **2006**, *45*, 4562.

44. Oh, E.; Hong. M. Y.; Lee, D.; Nam. S. H.; Yoon, H. C.; Kim, H. S. *J. Am. Chem. Soc.* **2005**, *127*, 3270.

45. (a) Huang, T.; Murray, R. W. *Langmuir* **2002**, *18*, 7077. (b) Hunag, C. C.; Chang, H. T.; *Anal. Chem.* ***2006***, *78*, 8332. (c) He, X. R.; Liu, H. B.; Li, Y. L.; Wang, S.;

Li, Y. J.; Wang, N.; Xiao, J. C.; Xu, X. H.; Zhu, D. B. *Adv. Mater*. **2005**, *17*, 2811.

46. (a) Chen, S. J.; Chang, H. T. *Anal. Chem.* **2004**, *76*, 3727. (b) Zhang, N.; Liu, Y. Y.; Tong, L. L.; Xu, K. H.; Zhuo, L. H.; Tang, B. *Analyst* **2008**, *133*, 1176.

47. (a) Bhandari, S.; Deepa, M., Sharma, S. N.; Joshi, A. G.; Srivastava, A. K.; Kant, R. *J. Phys. Chem. C* **2010**, *114*, 14606. (b) Bhattacharyya, S.; Sen, T.; Patra, A. *J. Phys. Chem. C* **2010**, *114*, 11787. (c) Sun, D.; Gang, O. *J. Am. Chem. Soc.* **2011**, *133*, 5252.

48. Brust, M.; Walker, M.; Bethell, D.; Schiffrin, D. J.; Whyman, R. J. *Chem. Soc. Chem. Commun.* **1994**, 801.

49. (a) Brust, M.; Fink, J.; Bethell, D.; Schiffrin, D. J.; Kiely, C. J.; Brust, M. *Chem. Soc. Chem Commun.* **1995**, 1655. (b) Kanaras, A. G.; Kamounah, F. S.; Schaumburg, K.; Kiely, C. J.; (c) Brust, M. *Chem. Commun.* **2002**, 2294. (d) Zheng, M.; Li, Z. G.; Huang, X.Y. *Langmuir* **2004**, *20*, 4226.

50. Bhattacharya, S.; Sen, T.; Patra, A. *J. Phys. Chem. C*. **2010**, *114*, 11787. (b) Bhandari, S.; Deepa, M.; Sharma, S. N.; Joshi, A. G. *J. Phys. Chem. C* **2010**, *114*,14606.

51. Clapp, A. R.; Medintz, I.; Mattoussi, H. *Chem. Phys. Chem*. **2006**, *7*, 47.

52. (a) Haldar, K. K.; Tapasi, S.; Patra, A. *J. Phys. Chem.* **2010**, *114*, 4869. (b) Li, M.; Cushing, S. K.; Wang, Q.; Shi, X.; Hornak, L. A.; Hong, Z.; Hu, N. *J. Phys. Chem. Lett.* **2011**, *2*, 2125.

53. (a) Tang, R.; Lee, H.; Achilefu, S. *J. Am. Chem. Soc*. **2012**, *134*, 4544. (b) Berezin, M. Y.; Achilefu, S. *Chem. Rev.* **2010**, *110*, 2641.

54. Park, Y.; Taranekar, P.; Park, J. Y.; Baba, A.; Fulghum, T.; Ponnapati, R.; Advincula, R.C. *Adv. Funct. Mater.* **2008**, *18*, 2017.

Chapter 2. Synthesis of Gold Nanoparticle-cored Polyamido Amine Dendrimer with Carbazole Functionalized Surface

2.1. Introduction

Nanoparticles with unique functionalities have drawn much interest in both academic and industrial fields as they are found to be potentially useful in many biological, chemical, and catalytic reactions.[1] The electronic and optical properties of the nanoparticles make them ideal candidates for use and fabrication in small electronic devices, or as chemical sensors and biosensors, and for drug delivery.[2] Apart from their innate properties, these nanoparticles are further functionalized by the ligands that stabilize them and thus customize their solubility, rigidity, and processability.[3]

Among the many ligands that stabilize nanoparticles, dendrimers are of high interest compared to the linear stabilizers. It has been shown that dendrimers produce more monodispersed nanoparticles and provide less diffusion of ions into the nanoparticles thus preventing agglomeration.[4] Dendrimers are architecturally special because they have a core which can be the main functional group that can stabilize the nanoparticle. They can be synthesized with increasing generation. They have surface functional groups that work to modify the surface chemistry of the nanoparticles which logarithmically increase in number as the generation increases. Lastly, the interior cavities of the dendrimer can serve as template or host for nanoparticle growth.[5] Dendrimer-encapsulated nanoparticles also called DENs have been extensively studied

for many areas of applications including: optoelectronic devices,[6] drug delivery[7] and plasmonic-based sensors,[8] and chemical catalysis.[9] The group of Crooks *et al.*[10] have pioneered the formation of metallic nanoparticles or nanoclusters using different generations of PAMAM dendrimers with varying surface functional group as the stabilizing agents for the immobilization of metallic nanoparticles such as gold, copper, and platinum. Generally in the synthesis of DENs, they pre-complex the dendrimer with metal ions that settle in the interior of the dendrimers. Upon addition of a reducing agent, the metal ions form the zero valent nanoparticles that reside in random cavities of the dendrimer. They are therefore immobilized and protected from aggregation with other metal ions.[9] In one of their studies, the groups of Crooks and Prato used DENs with gold nanoparticles as labeling agents for multi-walled carbon nanotubes.[10]

Another group of metal containing dendrimers well-studied by the group of Fox are the nanoparticle-cored dendrimers or NCDs where the core is a noble metal like gold nanoparticle[11] or palladium nanoparticle[12] and the dendrimers are actually dendron wedges with sulfide-containing focal point that self-assemble onto the surface of the gold nanoparticles. In both cases a modified Brust method of synthesizing gold or palladium nanoparticles was used wherein a chloride salt form of the gold or palladium is reduced by sodium borohydride ($NaBH_4$). This was then phase transferred into toluene using tetraoctylammonium bromide (TOAB) with Frechet-type dendrons having disulfide functionalities. In this study, they have found that the higher the generation of the dendrons used, the less the number of dendrons that self-assemble into the metal

nanoparticle core because of steric hindrance. Such ratio allows for a bigger surface area of the metal core exposed for use in catalysis as opposed to DENs. Although the synthesis using this method is efficient and facile, the removal of the TOAB is quite challenging as it ubiquitously appears in characterization despite several purification method. In a separate study,[13] Dihn *et al.* followed a convergent dendritic functionalization of a monolayered protected nanoparticles. In this work, gold nanoparticles stabilized by 11-mercaptoundecanoic acid (MUA) were conjugated to different genarations of Frechet-type dendrons with hydroxyl functional group using DCC/DMAP chemistry. In contrast to previous studies mentioned earlier, this method gives a superior control of the design parameter such as core size, dendron wedge density, and surface/interior functionality.

In a previous paper by our group, G4PAMAM dendrimer with amine functional group on the surface was functionalized with generational carbazole dendrons with carboxylic acid focal point to produce an electrochemically-cross-linked dendrimer.[14] Following this result in a separate work, π-conjugated terthiophene (PT) and carbazole (PC) dendrimers were used to functionalize a PAMAM dendrimer used as a redox nanoreactor to produce dendrimer-encapsulated metal nanoparticles (DEMNs) wherein the outer shell of electroactive dendrons served as reducing agents to the Au^{3+} ions complexed within the dendrimer to yield the zero valent gold nanoparticles.[15] The absorption and emission spectra of the dendrimers with AuNP showed an efficient energy transfer from the π-conjugation of the dendron ligands to the AuNPs facilitating

quenching of the emission. Another work from our group synthesized a nanoparticle-cored dendrimer using thiolated generational carbazole dendrons.[16] The carbazole dendrons with thiol focal point and Au^{3+} were dissolved in DDAB solution in toluene and upon addition of TOAB , the AuNPs were formed as evidenced by the change in color. They were stabilized by the thiol dendrons self-assembling onto the gold nanoparticle formed in-situ. The NCDs formed were electrochemically grafted on ITO substrate and spectroscopic analysis showed efficient energy transfer between the dendrons and the gold nanoparticles.

In this project we propose a facile synthesis of a nanoparticle-cored dendrimer with electroactive generation one (G-1) carbazole dendron from a generation three (G-3) cystamine-cored PAMAM dendrimer. The disulfide bond in the core of the PAMAM dendrimer is reduced to form the wedges or dendrons that stabilize the *in situ*-reduced gold nanoparticle. The current study provides a simple strategy to fabricating a dendron-stabilized Au nanoparticle (DSAuNPs) avoiding the stepwise and time-consuming anchoring of dendrons produced via a convergent approach. In this work we report the structural, spectroscopic and electrochemical properties of the DSAuNPs, and the energy transfer involved between the gold nanoparticle and the carbazole dendron.

2.2. Experimental Section

2.2.1. Materials

All chemicals were purchased from Alfa Aesar and were used directly without further purification. Tetrahydrofuran (THF) was freshly distilled over sodium and benzophenone before use. All solvents were aspirated with nitrogen gas before use. Cystamine-core generation three PAMAM dendrimer (G3PAMAM) with amine surface was purchased from Dentritech Nanotechnologies (DNT) Inc., (Midland, MI) in 20% (w/w) methanol solution. This was used without further purification and was dried by rotary evaporation.

2.2.2. Characterization

^{1}H NMR spectra were recorded using JEOL ECS 400 spectrometer (400 MHz). UV-Vis was recorded using Agilent 8453 Spectrometer. Fluorescence spectra were obtained using Perkin-Elmer LS45 luminescence spectrometer. Fluorescence lifetime decay was measured using PTI QuantaMaster(tm) Model QM-4 scanning spectrofluorometer with LaserStrobe utilizing 337.1 nm line N_2 laser pump. Data was analyzed using 1to 4 Exponential analysis. X-ray Photoelectron Spectroscopy (XPS) was done using a PHI 5700 X-ray photoelectron spectrometer equipped with a monochromatic Al Kα X-ray source (hν = 1486.7 eV) incident at 90^{o}, relative to the axis of a hemispherical energy analyzer. The spectrometer was operated both at high and low

resolutions with pass energies of 23.5 and 187.85 eV, respectively, a photoelectron take off angle of 45˚ from the surface, and an analyzer spot diameter of 1.1 mm. All spectra were collected at room temperature with a base pressure of 1 X 10^{-8} Torr. All the samples were completely dried in nitrogen gas prior to XPS measurements. Samples were prepared by spin casting onto a clean mica substrate. Cyclic voltammetry was performed using Autolab PGSTAT302 with GPES v4.9 program from Eco Chemie B.V. (Utrecht, The Netherlands) system with a three electrode cell. In all the measurements the counter electrode was platinum wire, Ag/AgCl as reference electrode, and ITO was used as working electrode. All FT-IR measurements were done on KBr pelletized samples using Digilab FTS 7000 step scan spectrometer. Transmission Electron Microscopy (TEM) images were taken using JEOL 1200CX operated at 80kV. TEM samples were prepared by drop casting dilute solution of G3PAMAM-NHCOG1Cbz-AuNP on 200-mesh copper grids coated with ultrathin lacey carbon film. The grids were placed in the vacuum oven overnight for complete drying before analysis.

2.2.3. Synthesis

Synthesis of 9-(4-bromobutyl)-9H-carbazole [CbzBr]. The synthesis of CbzBr was done by combining carbazole (20.64 g, 0.1234 mol), 1,4-dibromobutane (132 mL, 1.10 mol), tetrabutylammonium bromide (4.000 g, 0.01241 mol), toluene (200 mL), and 50% NaOH (200 mL). The resulting mixture was stirred at 45 ^{o}C for 3 hrs and continuously stirred at room temperature overnight. The clear, yellow organic layer was

then washed with 100-mL portions H_2O followed by 100 mL brine solution. This was then dried over anhydrous Na_2SO_4. The solvent was removed via rotary evaporator and the excess 1,4-dibromobutane via vacuum distillation. After which, the resulting cream-like solid residue was slowly dissolved in small portions of CH_2Cl_2. The yellow-brown solution was recrystallized using ethanol. The resulting white solid residue was dried under vacuum overnight with a yield of 88%. ^{1}H NMR (δ ppm in $CDCl_3$): 8.12 (d, *J*= 7.8 Hz, 2H), 7.22-7.48 (m, 6H), 4.36 (t, *J*= 6.88 Hz, 2H), 3.38 (t, *J*= 6.4 Hz 2H), 1.95-2.07 (m, 4H).

Synthesis of methyl 3,5-bis(4-(9H-carbazol-9-yl)butoxy)benzoate [G_1CbzCOOCH$_3$]. The synthesis of compound G_1CbzCOOCH$_3$ was done by combining CbzBr (27.93 g, 0.092 mol), methyl-3,5-dihydroxybenzoate (6.49 g, 0.039 mol), and 18-crown-6 (0.241 g) in acetone. To the resulting yellow solution mixture was added K_2CO_3 (29.46 g) and this was left at reflux for 3 days. The solvent was then removed using a rotary evaporator and the desired compound extracted with CH_2Cl_2. The organic layer was subjected to rotary evaporation until 20-25 mL was left just to dissolve the solid residue. Ethyl acetate was used to precipitate out the desired white solid compound with a yield of 76 %. ^{1}H NMR (δ ppm in $CDCl_3$): 8.10-8.08 (d, *J*= 7.76 Hz, 2H), 7.45-7.340 (m, 8H), 7.25-7.20 (m, 7H), 6.54-6.53 (t, *J*= 4.6 Hz, 1H), 4.41- 4.38 (t, *J*= 7.36, 4H), 3.96-3.93 (t, *J*= 5.96, 4H), 2.11-2.04 (m, 4H), 1.87- 1.80 (m, 4H), 1.5 (s, 2H).

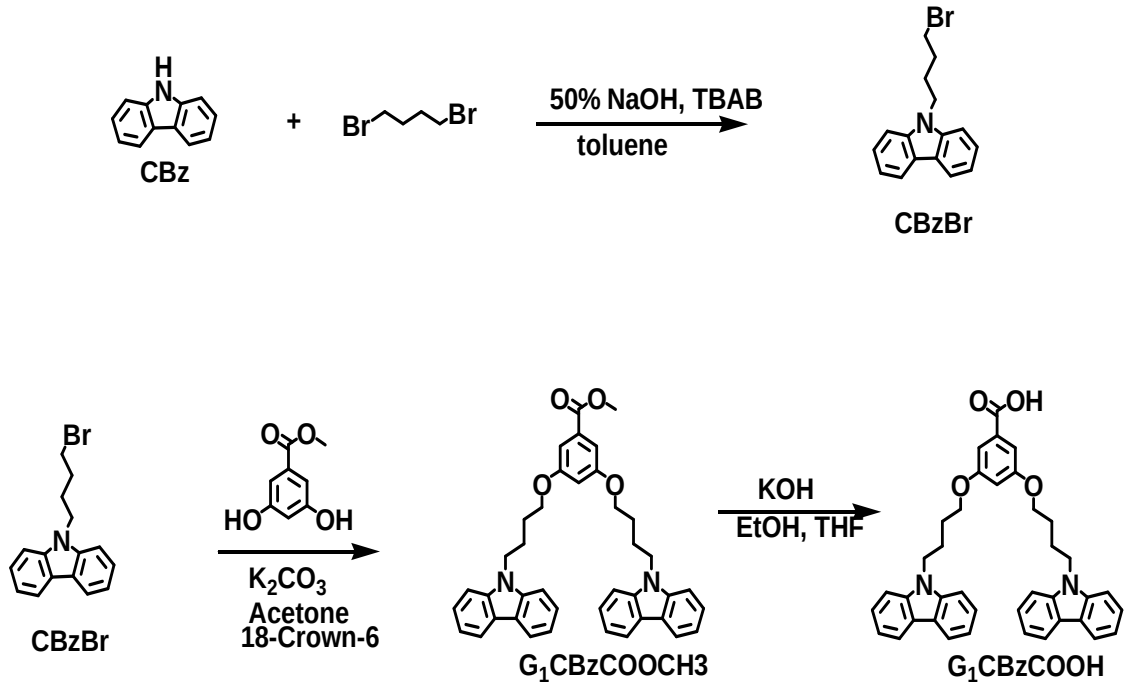

Scheme 2.1. Synthesis of G_1CBzCOOH by simple hydrolysis.

Synthesis of 3,5-bis(4-(9H-carbazol-9-yl)butoxy)benzoic acid [G_1CbzCOOH].

To afford the carboxylic acid form of generation one carbazole dendron, $G_1CbzCOOCH_3$ (4.000 g, mol) was dissolved in 30:20 THF:ethanol. To the mixture was added KOH in a 1:10 ratio (3.840 g) dissolved in 1 mL MilliQ water. After 48 hours of reflux, the reaction mixture was cooled to room temperature and acidified to pH 2-3 with dropwise addition of concentrated HCl. The white precipitate was filtered out and purified through silica gel column with 5% MeOH:CH_2Cl_2 as eluent. The yield was 50%. ^{1}H NMR (δ ppm in $CDCl_3$): 8.09 (d, *J* = 7.8 Hz, 4H), 7.84-7.39 (m, 8H), 7.24-7.17 (m, 4H), 7.16 (s, 2H),

6.57 (s,1H), 4.40 (t, *J* = 6.3 Hz, 4H), 3.94 (t, *J* = 6.0 Hz, 4H,), 2.08 (m, 4H), 1.84 (m, 4H).

Synthesis of G3PAMAM-NHCOG$_1$CBz. The amine terminated, cystamine-core, G3–polyamido amine dendrimer (G3PAMAM) has 32 primary amines on the surface. These amines were conjugated with carbazole dendrons with carboxylic acid moiety using EDC/DMAP chemistry as previously reported by our group.[14] Briefly, 100 mg of G3PAMAM-NH_2 was dissolved in dry DMF under nitrogen to which G_1CBzCOOH in DMF was added in a 1:50 ratio. The amidation reaction was followed through by slow addition of EDC in DMF under nitrogen. A solution of DMAP in dry DMF was added dropwise through a syringe in a 3:1 ratio with EDC. After 48 hours stirring at room temperature, the amide product, G3PAMAM-NHCOG$_1$CBz, was purified through glass support silica plates using 10% MeOH/ CH_2Cl_2 as eluent with a yield of 25%. The clear oily product was analyzed using ^{1}H NMR and FTIR spectra using the KBr method. ^{1}H NMR (δ ppm in dDMSO): 8.11-8.09 (d, *J* = 7.4 Hz, 4H), 7.58-7.57 (d, *J* = 8.0, 4H), 7.41-7.38 (t, *J* = 1.15 Hz, 4H), 7.15-7.13(t, *J* = 6.8 Hz, 4H), 6.49-6.48 (m, 3H), 6.46-6.45 (t, *J* = 2.3 Hz, 1H), 4.44-4.42 (t, *J* = 6.9 Hz, 4H), 4.12-4.11 (d, *J* = 4.65 Hz, 111H), 3.89-3.88 (t, *J* = 6.3 Hz, 4H), 3.13-3.12 (m, , 210 H), 2.85 (s, 2H), 2.7 (s, 2H), 2.47-2.46 (m, 14H), 2.19-2.17 (d, *J* = 7.45 Hz, 4H).

Synthesis of G3PAMAM-NHCOG$_1$CBz stabilized AuNPs. Synthesis of the PAMAM-carbazole-stabilized gold nanoparticles was done using a modified version of a previously reported method.[17] Briefly 50 mg of G3PAMAM-NHCOG$_1$CBz and 80 mg of

$NaBH_4$ was dissolved in 25 mL degassed DMSO to reduce the disulfide bond. This was allowed to stir under nitrogen for 2 hour. To this reaction mixture was added 1 mL of $HAuCl_4$ solution in DMSO (99 mg/50 mL DMSO). The reaction immediately turned dark blue and was allowed to react for 24 hours under nitrogen. The nanoparticles were precipitated with acetonitrile and were centrifuged at 4000 rpm for 10 minutes. The dark pellets were re-dispersed and centrifuged in 1:1 acetonitrile:DMSO, then 50 mL ethanol, and lastly 50 mL diethyl ether. The desired product was dried under nitrogen in vacuum.

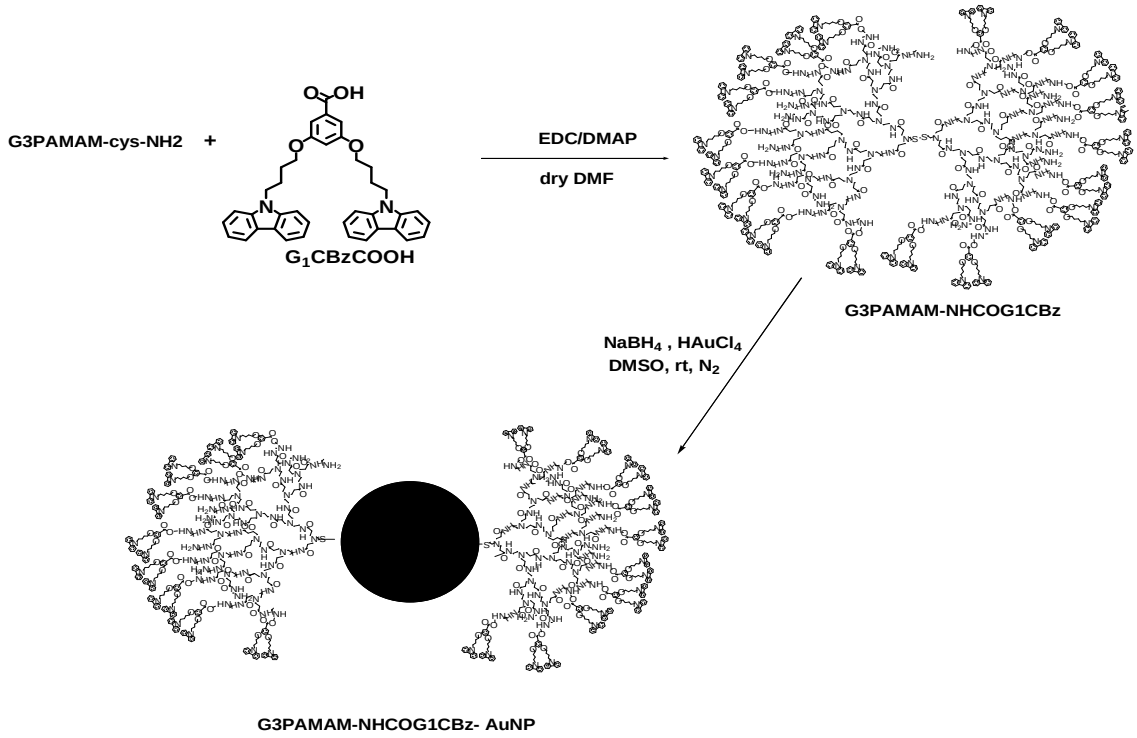

Scheme 2.2. Synthesis of G3PAMAM-NHCOG_1CBz stabilized AuNPs. The amine group of PAMAM form an amide bond with the carboxylic acid-functionalized carbazole dendrons. The disulfide bond of the PAMAM core is reduced by $NaBH_4$.

2.3. Results and Discussion

2.3.1. Synthesis and Characterization

The amine terminated, cystamine-cored, G3PAMAM dendrimers were conjugated with generation one carboxylic acid functionalized Frechet-type polyarylether dendrons (G1CBzCOOH) using EDC/DMAP chemistry to form an amide functional group. Scheme 2.2 shows a scheme of the synthesis of the disulfide-cored G3PAMAM dendrimer whose amine surface is functionalized with conjugated carbazole dendrons.

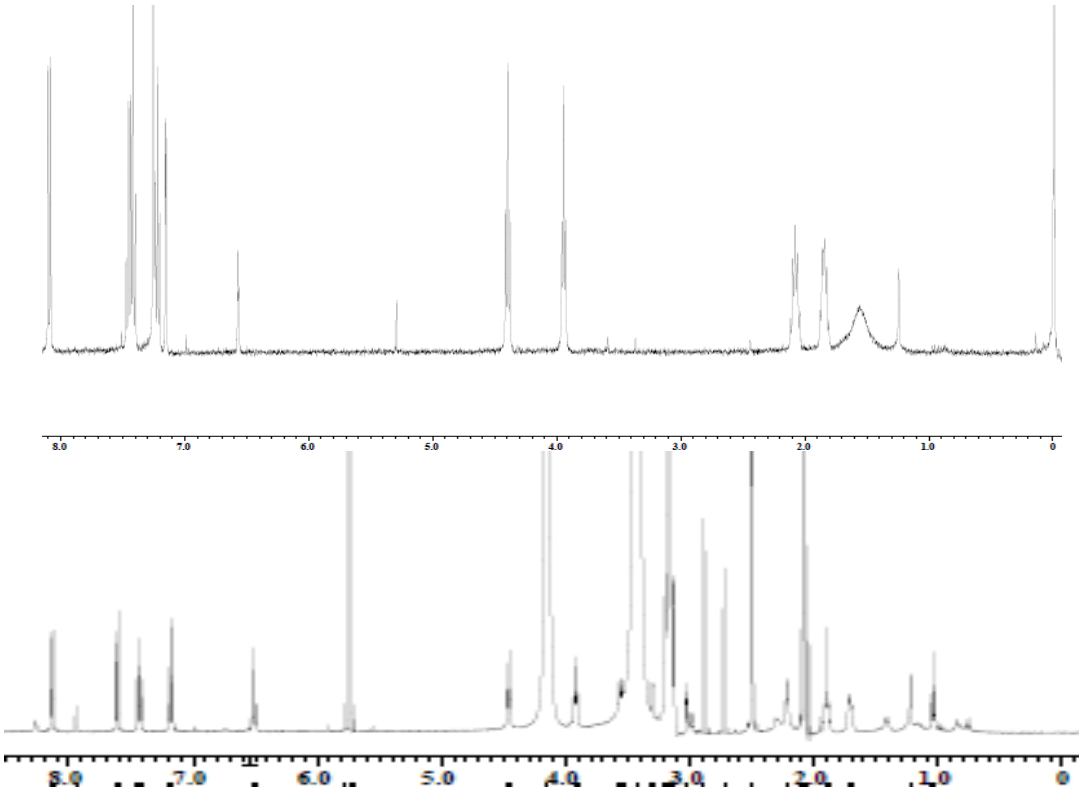

Figure 2.1. ^{1}H NMR spectra of G1CBzCOOH (top) and G3PAMAM-NHCOG1CBz (bottom). The shifts at 3.15 ppm for N-CH_2 protons indicate presence of PAMAM dendrimer.

Figure 2.1 shows the HNMR spectra of the carbazole dendron with carboxylic acid moiety and of the PAMAM conjugated with carbazole. The characteristic peaks found at 8.1 ppm and 7.4-7.6 ppm assigned to the aromatic protons of the carbazole ring and peaks at 3.9 and 4.4 ppm assigned to the CH_2 aliphatic protons of the carbazole moiety verifies the addition of the carbazole units to the G3PAMAM dendrimer. The 7.9 singlet peak can be assigned to the amine group of the PAMAM. The proton peak with 3.15 ppm is assigned to N-CH_2 protons. The peaks assigned to the carbazole and PAMAM units were consistent with reported values in the literature.[18]

The PAMAM-carbazole dendrimer was also characterized using FT-IR spectroscopy. As seen on the spectra in Figure 2.2b, the shift to a lower wavenumber of the C=O stretch from 1692 cm^{-1} to 1647 cm^{-1} indicates the formation of the amide bond upon conjugation with the amine group of PAMAM. The characteristic absorptions of amide bonds appear at 1647 cm^{-1} and 1569 cm^{-1} for amide I and II modes.[19] In addition, peaks were observed at 3390 for N-H stretch, 3047 cm^{-1} for antisymmetric N-H stretch for primary amine, 2942 cm^{-1} for aliphatic C-H stretch, 1436 cm^{-1}, and 1395 cm^{-1} for N-H bending for N-substituted amide.

The presence of the carbazole is also seen at 1334 C-N stretching at the ring of the carbazole, and 1421 for C=C present in the aromatic ring of the carbazole. The peak in the 3500-3300 cm^{-} in Figure 2.2(b) suggests the N-H stretching in the PAMAM group which shows that some of the amine bonds did not react with the –COOH group of the carbazole probably because of steric hindrance.[14]

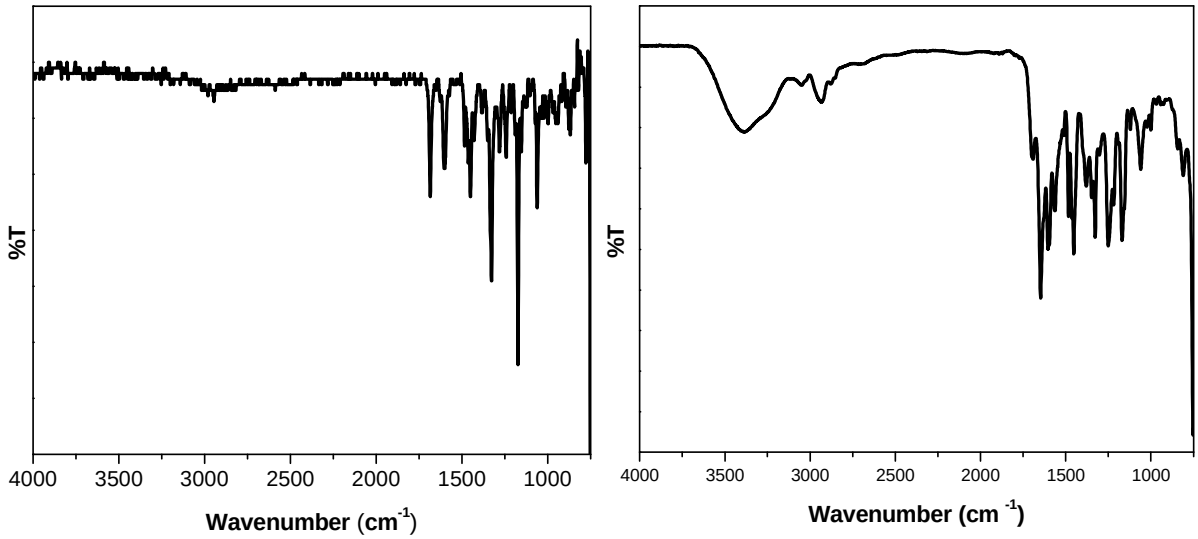

Figure 2.2. IR spectra of (a) G1CBzCOOH and (b) PAMAM-NHCOG1CBz showing the formation of amide bond. The shifting of the C=O bond from 1692 cm^{-1} to 1647 cm^{-1} shows formation of amide bond.

The G3PAMAM-NHCOG1CBz dendrimer was dissolved in DMSO and was allowed to react with an excess amount of sodium borohydride to cleave the disulfide bond in the core of the dendrimer. After two hours stirring at room temperature under nitrogen, a solution of $HAuCl_4$ in DMSO was added rapidly into the reducing mixture and the clear solution instantly turned dark brown to purplish shade and the reaction was allowed to proceed for 24 hours. The change in color indicated the formation of gold nanoparticles.[11,15]

2.3.2. X-ray Photoelectron Spectroscopy

The formation of elemental gold, Au(0) was analyzed through X-ray photoelectron emission spectroscopy. Figure 2.3 shows the characteristic $4f^{7/2}$ and $4f^{5/2}$ spin-orbit doublet XPS peaks of Au(0) with binding energy of 88.05 eV and 84.38 eV, respectively separated by 3.67 eV. The broadness of the peaks indicate the presence of other possible gold species which may be attributed to some gold ions that were not completely reduced as can be seen from the image in Figure 2.3 (a) where an extrapolation of the peaks shows another doublet peaks at higher binding energies of 88.47 eV and 84.80 eV corresponding to the $4f^{7/2}$ and $4f^{5/2}$ spin-orbit doublet peaks of gold ions (Au^{3+}).[20] This is in agreement with XPS data for self-assembled alkanedithiol and alkanethiol on AuNPs as well as bulk gold substrates.[20] Likewise the deconvolution of the broad peak for the XPS spectra of sulfur in Figure 2.3(b) shows the binding energies of sulfur in the spin-orbit doublet S $2p^{3/2}$ and S $2p^{1/2}$ separated by 1.17 eV. The binding energy values at 161.53 eV and 162.71 eV corresponds to the S $2p^{3/2}$ and S $2p^{1/2}$ respectively further confirming the formation of Au-S bond.[21] The 164.26 eV binding energy for S $2p^{3/2}$ corresponds to free thiol or unbound sulfur.[22]

2.3.3. UV Absorption and Luminescent Properties

To further assess the formation of the AuNPs decorated with the carbazole-functionalized PAMAM cystamine dendrons, UV-vis and emission data were collected.

The characteristic peaks of the carbazole dendrons at 329 nm and 343 nm correspond to π-π^* and n-π^* electronic transitions respectively[23] as seen in the UV absorbance spectra in Figure 2.4(a). Upon formation of gold nanoparticles the peaks at 329 nm and 343 nm are still apparent followed by a broadening of the tail, a very slight shift to longer wavelength which may indicate an oxidation process and *in-situ* cross-linking of the carbazole dendrons upon reduction of Au^{3+} to Au(0).[16] The formation of the AuNPs is evidenced by the absorbance peak centered around 550 nm corresponding to the surface plasmon resonance characteristic of gold nanoparticles.[14] It is interesting to note the appearance of a broad band extending to 710 nm which can be assigned to the π–π^* transitions of the 3,3'-dicarbazyl dication (bipolaronic band or more highly doped state) further confirming the in-situ cross-linking of the carbazole species.[14,24]

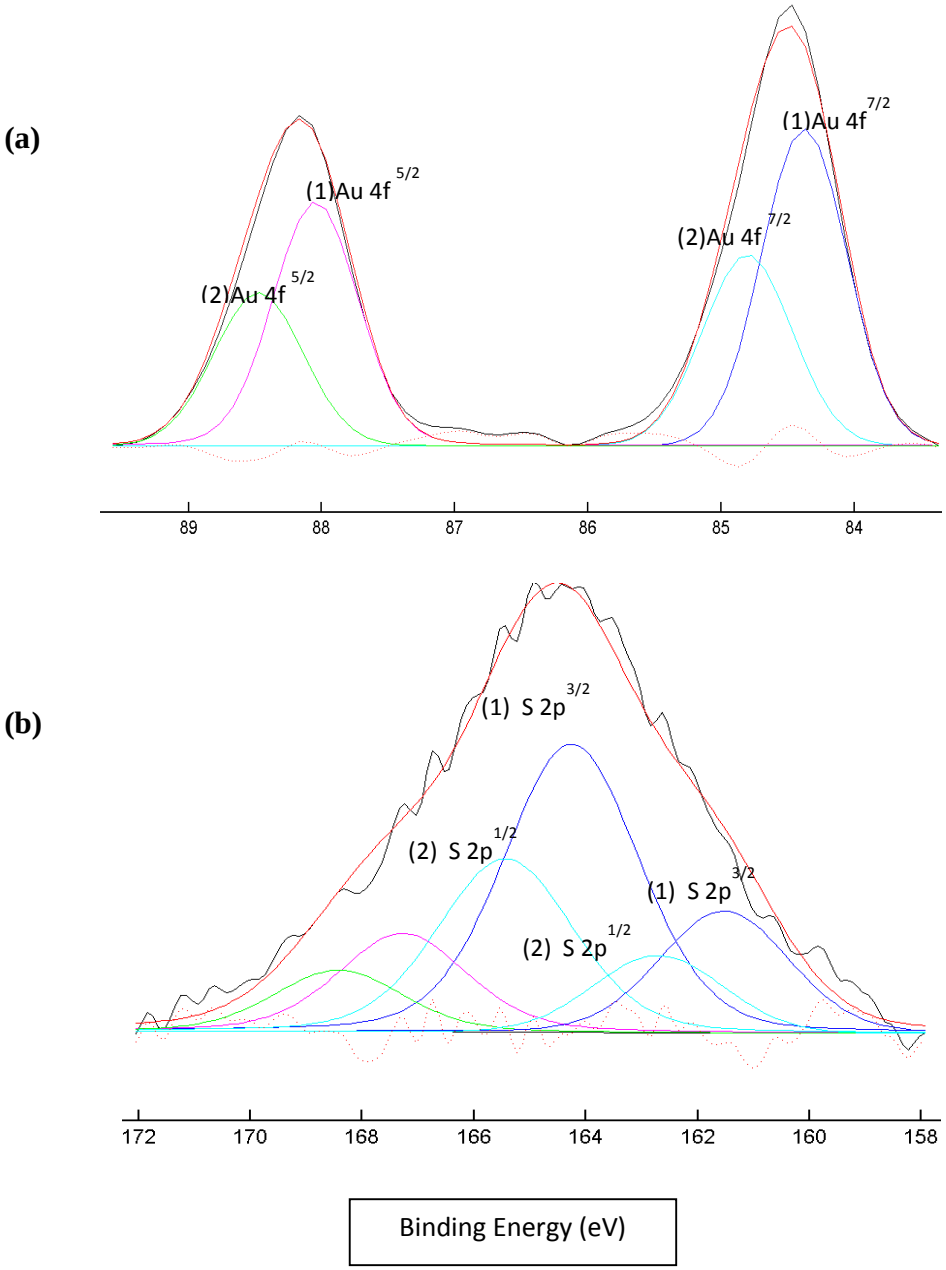

Figure 2.3. XPS data of (a) Au(0) at peaks (1) and Au^{3+} at peaks (2) and (b) S as bound to Au at peaks (1) and as free or unbound thiol at peaks (2). Presence of S-Au bond indicates the reduction of PAMAM disulfide bond and stabilization of AuNPs by the dendrons.

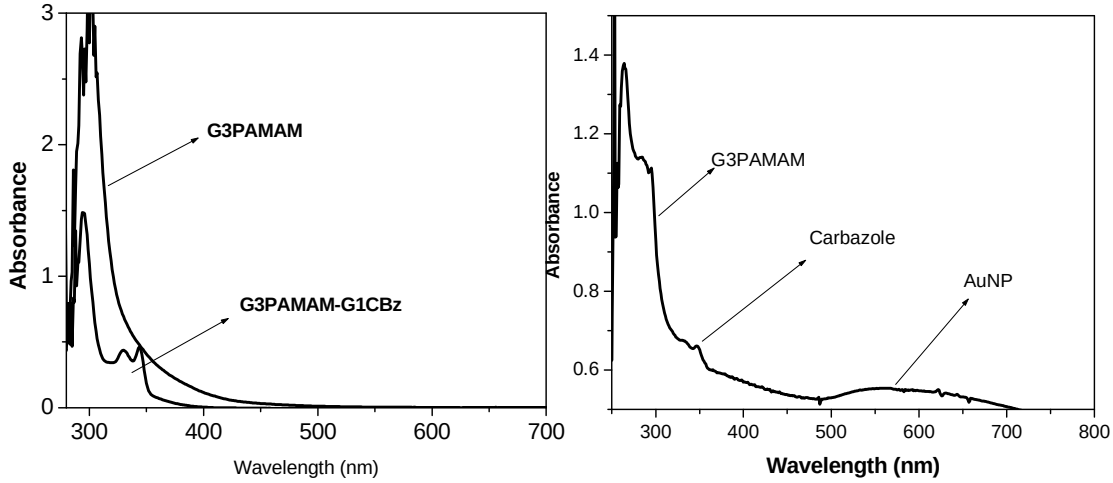

Figure 2.4. Absorbance spectra of (a) G3PAMAM and G3PAMAM-NHCOG1CBz and (b) the gold nanoparticle-cored dendrimer showing peaks for G3PAMAM-NHOG1CBz with surface plasmon resonance peak.

The photoluminescence spectra of both the dendrimer with and without the AuNPS showed a prominent peak at 370 nm corresponding to the carbazole emission. The fluorescence emission intensities of the G3PAMAM-NHCOG1CBz with and without AuNP are shown in Figure 2.5 where the peak for the dendrimer alone has a maximum at 370 nm. But the maximum peak for the dendrimer with AuNP shows a red shifting to 382 nm with a prominent shoulder at 392 nm. This bathochromic shift which is also seen in the absorbance spectra suggests a possible cross-linking of the carbazole moiety upon reduction of Au^{3+} as well as energy transfer between the carbazole units and the gold nanoparticles. This energy transfer can also be manifested by the change in the fluorescence lifetime of the excited molecule. The increase in the rate of decay of the dendrimer with the AuNP is shown in Figure 2.6 where the lifetime decreased from 3.67

ns (a) to 2.82 ns (b) in the presence of AuNPs . Such change in the excitation lifetime of the molecule suggests a non-radiative energy transfer from the carbazole to the gold nanoparticles.[25]

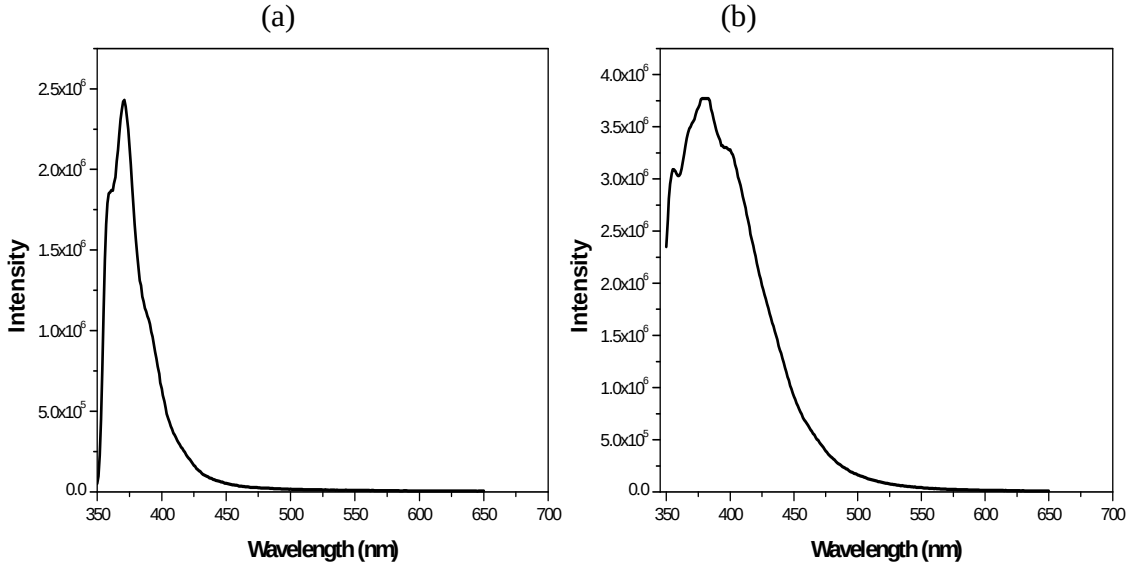

Figure 2.5. Emission spectra of G3PAMAMNHCO-G1CBz without (a) and with (b) AuNP excited at 337 nm in DMSO solution. Shoulder at 425 nm (b) in the presence of AuNP suggests crosslinking of carbazole upon reduction of Au^{+3}.

2.3.4. Cyclic Voltammetry by Electrodeposition

The synthesis of DSAuNPS that are cross-linkable provides a way to facilitate the energy transfer between the gold nanoparticles and the electroactive dendrons. To study the electrochemical behavior of the dendrimer, electrochemical oxidative cross-linking was performed on an previously cleaned ITO-coated glass substrates.[14] The nanoparticles in DMSO were dropcast onto the clean ITO substrates and were dried in the vacuum

oven overnight to form optically transparent thin film. A three-electrode cell was constructed with 0.1M tetrabutyl ammonium hexafluorophosphatee (TBAH) in acetonitrile with Pt wire used as counter electrode, and Ag/AgCl as reference electrode. The potential range used was 0 V to 1.2 V using 10 cycles with a scan rate of 50 mV/s.

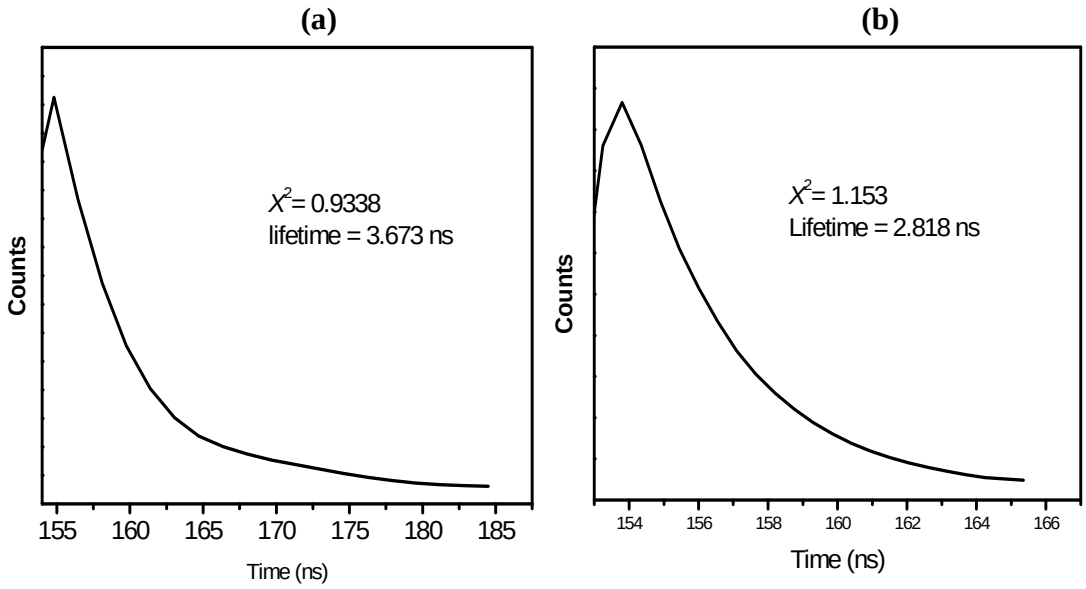

Figure 2.6. Fluorescence lifetime of (a) G3PAMAM-NHCOG1CBz and (b) G3PAMAM-NHCOG1CBz-AuNP in DMSO solution with λ_{exc} = 337 nm using 1to 4 exponential analysis. The presence of AuNP shows a decrease in the fluorescence lifetime of the nanoparticle suggesting energy transfer from π-conjugated carbazole to AuNP.

The cyclic voltammogram (CV) traces of the electrodeposition of G3PAMAM-NHCOG1CBz and G3PAMAM-NHCOG1CBz-AuNP on ITO-coated glass are shown in Figure 2.7. From the cyclic voltammogram, the strong peaks centered at 0.70 V and 1.0 V (vs Ag/AgCl) are due to the oxidation of the polycarbazole. The characteristic oxidation peak at 1.0 V for the formation of polycarbazole species is seen

in both. Interestingly however, the presence of the AuNP facilitated a more favorable cross-linking of the carbazole species as can be seen in the appearance of the oxidation peak at 0.7 V. The CV diagrams give a clear evidence of the electrochemical cross-linking of the available free carbazole units attached to the PAMAM dendrons. This represents the generation of radical cation species that lead to coupling of carbazoles at the 3,6-position and subsequent oligomerization.

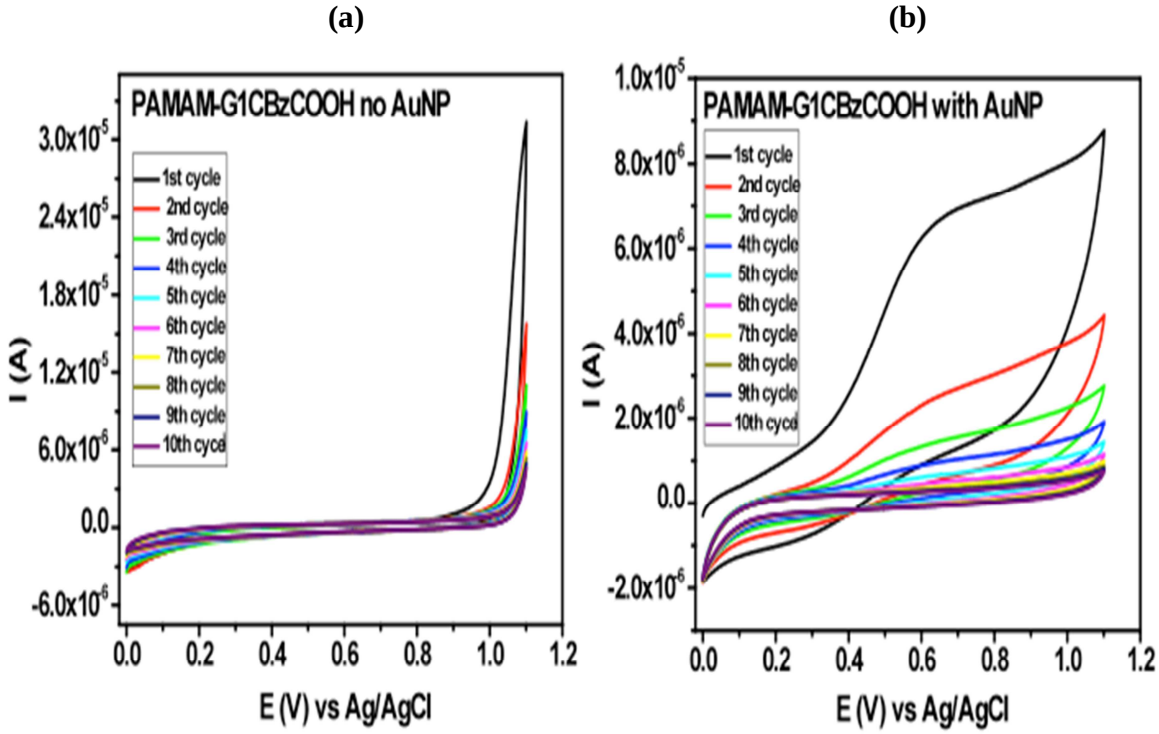

Figure 2.7. Cyclic voltammograms of (a) G3PAMAM-NHCOG1CBz without AuNP and (b) G3PAMAM-NHCOG1CBz with AuNP. Presence of AuNP shows shifting of oxidation potential. The ability to crosslink the carbazole electrochemically is retained.

2.3.5. Transmission Electron Microscopy

Further characterization of the formation of the DSAuNPs is shown in the transmission electron micrograph in Fig. 2.8. showing a well-dispersed nanoparticle distribution in the organic solvent without any fused particles. These nanoparticles are seen as spherical in shape with an average diameter size of 4.11 nm. The large spaces between the nanoparticles suggest the presence of large dendrimers surrounding the particles preventing fusing or aggregating.

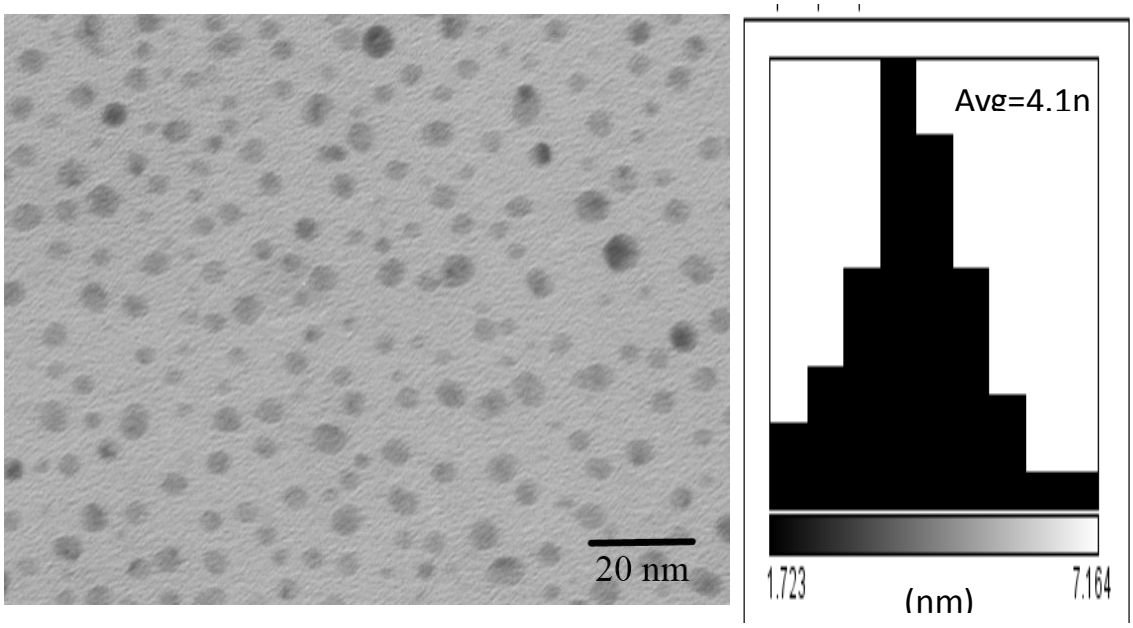

Figure 2.8. Representative Transmission Electron Microscopy image of the G3PAMAM-NHCOG1CBz-AuNP at 200k X magnification and histogram of the size distribution with an average of 4.1 nm. Wide distance between AuNPs indicate stabilization by large G3PAMAM-NHCOG1CBz dendrons

This reported size is larger compared to those described in the work by Crooks where they made DENs using PAMAM dendrimers as template.[9d] This average size is close to those described in G4-PAMAM dendrimers (about 4.5 nm).[25] However given this large size in G3-PAMAM dendrimers, it is less likely that these nanoparticles are in the interior cavities of the dendrimer but instead represent the core of the dendrimer.[17] The self-assembly of the Au-S bond from the dendron wedges predominates the stability and immobilization of the nanoparticles thus forming the nanoparticle-cored dendrimer.

2.4. Conclusions

Nanoparticle-cored dendrimer was synthesized using a facile direct synthesis method wherein carbazole-capped G3PAMAM dendrimer was cleaved along its disulfide core to form the thiolated dendrons that were used to stabilize the formation of gold nanoparticles. Spectroscopic analysis showed a surface plasmon band with absorbance centered at 550 nm. FTIR spectra showed amide bond formation upon esterification reaction of the amine surface of the PAMAM dendrimer with the carboxylic acid functionalized generation one carbazole dendrons to give an amide bond. Photoluminescence shows a slight shifting of the emission peaks to higher wavelength energy and an energy transfer mechanism in-effect between gold nanoparticles and carbazole units. This is evidenced by the increase in the rate of decay of the fluorescence lifetime of the dendrimer with AuNP as the latter acts as a fluorescence quencher. The dendrimer synthesized in this work is electroactive imparting this hybrid nanoparticle

more rigidity and stability. TEM image shows the formation of the nanoparticles with a broader histogram and larger size than encapsulated DENs and DEMNs. Future study will focus on a more qualitative charge transfer and energy transfer properties of this hybrid material.

2.5. References

1. (a) Daniel, M. C.; Astruc, D. *Chem. Rev.* **2004**, *104*, 293. (b) Niu, Y.; Yeung, L.K.; Crooks, R. M. *J.Am.Chem.Soc.* **2001**, *123*, 6840.
2. (a) Dasary, S. S. R.; Singh, A. K.; Senapati, D.; Yu, H.; Ray, P. C. *J. Am. Chem. Soc.* **2009**, *131*, 13806. (b) Beqa, L.; Singh, A. K.; Khan, S. A.; Senapati, D.; Arumugan, S. R. Ray, P. C. *ACS Appl. Mater. Interfaces* **2011**, *3*, 668. (c) McNicholas, T. P.; Zhao, K.; Yang, C.; Hernandez, S.; Mulchandani, A.; Myung, N. V.; Deshusses, M. A. *J. Phys. Chem. C* **2011**, *115*, 13927. (d) Jaramillo, T.; Baeck, S. H.; Cuenya, B. R.; McFarland, E. *J. Am. Chem. Soc.* **2003**, *125*, 7148.
3. (a) Astruc, D.; Boisselier, E.; Ornelas, C. *Chem. Rev.* **2010**, *110*, 1857. (b) Schulz-Dobrick, M.; Sarathy, K. V.; Jansen, M. *J. Am. Chem. Soc.* **2005**, *127*, 12816. (c) Lin, S. Y.; Tsai, Y. T.; Chen, C. C.; Lin, C. M.; Chen, C. *J. Phys. Chem. B* **2004**, *108*, 2134.
4. (a) Bronstein, L.; Shifrina, Z. *Chem. Rev.* **2011**, *111*, 5301. (b)Esumi, K.; Suzuki, A.; Yamahira, A.; Torigoe, K. *Langmuir* **2000**, *16*, 2604. (c) Crooks, R. M.; Zhao, M.; Sun, L.; Chechik, V.; Yeung, L.K. *Acc. of Chem. Res*. **2001**, *34*, 181.
5. (a) Huang, B.; Tomalia, D. A. *Journal of Luminescence,* **2005**, *111*, 215. (b) Tomalia, D. A; Naylor, A. M ; Goddard, W. A, III *Angew. Chem. Int. Ed. Engl.* **1990**, *29*, 138. (c) Tomalia, D. A, Baker, H. ; Dewald, J.; Hall, M.; Kallas, G.; Martiin, S.; Roeck, J.; Ryder, J. ; Smith, P. *Polym. J.* **1985**, *17*, 117. (d)

Newkome, G. R.; Yao, Z. Q.; Baker, G. R.; Gupta, V. K. *J. Org. Chem*. **1985**, *50*, 2003.

6. (a) Fosdick, S. E.; Crooks, R. M. *J. Am. Chem.Soc.* **2012**, *134*, 863. (b) Gittins, D. I.; Bethell, D.; Schiffrin, D. J.; Nichols, R. J. *Nature* **2000**, *408*, 67. (c) Hiroshi, S.; Yamamoto, Y.; Yakabe, H.; Tokonami, S.; Nagaoka, T. *Chem.Commun.* **2003**, 1038.
7. (a) Umeda, Y.; Kojima, C.; Harada, A.; Horinaka, H.; Kono, K. *Bioconjugate Chem.* **2010,** *21,* 1559. (b) Wang, Y.; Kong, W.; Song, Y.; Duan, Y.; Wang, L.; Steinhoff, G.; Kong, D.; Yu, Y. *Biomacromolecules* **2009**, *10*, 617.
8. Yao, J.; Le, A. P.; Schulmerich, M. V.; Maria, J.; Lee, T. W.; Gray, S. K.; Bhargava, R.; Rogers, J. A.; Nuzzo, R.G. *ACS Nano* **2011**, *5*, 5763.
9. (a) Gomez, M. V.; Guerra, J.; Velders, A. H.; Crooks, R. M. *J. Am. Chem. Soc.* **2009**, *131*, 341. (b) Scott, R. W. J.; Wilson, O. M.; Crooks, R. M. *J. Phys. Chem. B* **2005**, *109,* 692. (c) Knecht, M. R.; Garcia-Martinez, J. C.; Crooks, R. M. *Langmuir* **2005**, *21,* 11981. (d) Kim, Y. G.; Oh, S. K.; Crooks, R. M. *Chem. Mater*. **2004**, *16*, 167.
10. Herrero, M. A.; Guerra, J.; Myers, V. S.; Gomez, M. V.; Crooks, R. M.; Prato, M. *ACS Nano* **2010**, *4*, 905.
11. (a) Gopidas, K. R.; Whitesell, J. K.; Fox, M. A. *J. Am. Chem. Soc.* **2003**, *125*, 6491. (b) Gopidas, K. R.; Whitesell, J .K.; Fox, M. A. *J. Am. Chem. Soc*. **2003**, *125*, 14168.

12. Gopidas, K. R.; Whitesell, J. K.; Fox, M. A. *Nano Lett.* **2003**, *3*, 1757.

13. Shon, Y. S.; Choi, D.; Dare, J.; Dinh, T. *Langmuir* **2008**, *24*, 6924.

14. Kaewtong, C.; Guoqian, J.; Felipe, M. J.; Pulpoka, B.; Advincula, R.C. *ACS Nano* **2008**, *2*, 1533.

15. Kaewtong, C.; Guoqian, J.; Ponnapati, R.; Pulpoka, B.; Advincula, R.C. *Soft Matter* **2010**, *6*, 5316.

16. Danda, C.; Ponnapati, R.; Dutta, P.; Taranekar, P.; Patterson, G.; Advincula, R. C. *Macromol. Chem. Phys.* **2011**, *212*, 1600.

17. Villalonga, R.; Díez, P.; Casado, S.; Eguílaz, M.; Yañez-Sedeño, P.; Pingarrón, J. M. *Analyst* **2012**, *137*, 342.

18. (a) Yu, G. S.; Bae, Y. M.; Choi, H.; Kong, B.; Choi. I.S.; Choi, J. S. *Bioconjugate Chem.* **2011**, *22*, 1046. (b) Huang, J. F.; Luo, H.; Liang, C.; Sun, I-W.; Baker, G. A.; Dai, S. *J. Am. Chem. Soc.* **2005**, *127*, 12784.

19. (a) Rousseau, G.; Fensterbank, H.; Baczko, K.; Cano, M.; Allard, E.; Larpent, C. *Macromolecules* **2012**, *45*, 3513. (b) Singh, P.; Gupta, U.; Asthana, A.; Jain, N. *Bioconjugate Chem.* **2008**, *19*, 2239.

20. (a) Joseph, Y.; Besnard, I.; Rosenberger, M.; Guse, B.; Nothofer, H. G.; Wessels, J. M.; Wild, U.; Knop-Gericke, A.; Su, D.; Schlogl, R.; Yasuda, A.; Vossmeyer, T. *J. Phys. Chem. B* **2003**, *107*, 7406. (b) Chenakin, S. P.; Heinz, B.; Morgner, H. *Surf. Sci.* **1999**, *421*, 337. (c) Castner, D. G.; Hinds, K.; Grainger, D.W.*Langmuir*

1996, *12*, 5083. (d) Heister, K.; Zharnikov, M.; Grunze, M.; Johansson, S. O. *J. Phys. Chem. B.* **2001**, *105*, 4058.

21. Mazzaglia, A.; Scolaro, L. M.; Mezzi, A.; Kaciulis, S.; DeCaro, T.; Ingo, G. M.; Padelletti, G. *J. Phys. Chem. C.* **2009**, *113*, 12772.

22. Wang, X.; Lieberman, M. *Langmuir* **2003**, *19*, 7346.

23. (a) Taranekar, P.; Fulghum, T.; Baba, A.; Patton, D.; Advincula, R. C. *Langmuir* **2007**, *23*, 908. (b) Taranekar, P.; Park, J. Y.; Patton, D.; Fulghum, T.; Ramon, G. J.; Advincula, R.C.*Adv. Mater*. **2006**, *18*, 2461.

24. Ambrose, J. F.; Nelson, R. F. R. *J. Electrochem. Soc.* **1968**, *115*, 1159.

25. (a) Sen, T.; Mandal, S.; Haldar, S.; Chattopadhyay, K.; Patra, A., *J. Phys. Chem C.* **2011**, *115*, 24037. (b) Gu, J. Q.; Shen, J.; Sun. L. D.; Yan, C.-H. *J. Phys.Chem. C* **2008**, *112*, 6589.

26. (a) Xia, C.; Advincula, R. C. *Chem. Mater.* **2001**, *13*, 1682.; (b) Ambrose, J. F.; Nelson, R. F. R. *J. Electrochem. Soc.* **1968**, *115*, 1159. (c) Mengoli, G.; Musiani, M. M.; Schreck, B. *J. Electroanal. Chem.* **1988**, *246*, 73. (d) Inzelt, G. *J. Solid State Electrochem.* **2003**, *7*, 503.

27. Crooks. R. M.; Zhao, M.; Sun, L.; Chechik, V.; Yeung, L. K. *Acc. Chem. Res.* **2011**, *34*, 181. (b) Tokuhisa, H.; Zhao, M.; Baker, L. A.; Phan, V. T.; Dermody, D.A.; Garcia, M. E.; Peez, R. F.; Crooks, R. M.; Mayer, T. M. *J. Am. Chem. Soc.* **1998**, *120*, 4492.

Chapter 3. Energy Transfer in Hybrid Dendron-capped CdSe Quantum Dots with *in-situ* Reduced Au Nanoparticles

3.1. Introduction

Hybrid metal-semiconductor nanoparticles have potential in variety of applications such as solar energy conversion,[1] electronic devices,[2] biological imaging and sensors,[3] and photocatalysis.[4] The interesting interplay of their spectral properties, that is, the localized surface plasmon resonance of the metal nanoparticle (e.g. AuNPs)[5] and the highly fluorescent and photostable semiconducting quantum dots (e.g. CdSe)[6] have led to several reports on the coupling of metallic nanoparticle and fluorescent quantum dots.[8] The coupling of these two nanoparticles resulted to size- and shape-tunable electronic and optical properties. This is mainly attributed to the quantum confinement effect for the quantum dots which is the increase in the HOMO-LUMO gap as the size of the crystal decreases[7] and the dielectric confinement or plasmon resonance of the metallic nanoparticles that causes high polarizability at the frequency of the plasmon band.[8]

The energy transfer interaction between semiconducting, highly fluorescent CdSe quantum dots (QD) and plasmonic Au nanoparticles (Au-NPs) can either be attenuated or enhanced depending on their spatial proximity or spectral overlap.[9] Due to the unique spectroscopic properties of highly luminescent QDs, they have become efficient donors for energy transfer assays both for optoelectronics and biological imaging studies.[10] In the presence of nearby Au-NPs however, a quenching of the fluorescence of the QDs or a

dye may occur due to a non-radiative energy transfer pathway from the fluorescent donor to the metal. These observed properties make QDs and AuNPs good donor-acceptor pairs in energy transfer mechanism studies such as Förster Resonance Energy Transfer (FRET) and nanoparticle surface energy transfer (NSET).[10] The energy transfer is evidenced by quenching through steady state fluorescence spectroscopy or by fluorescence lifetime decay.

The synthetic structure of this kind of hybrid nanoparticle have been reported in different architectures like QDs directly situated on the surface of AuNPs as core-shell structure or vice versa,[11] or CdSe connected to the AuNP by linear organic polymers,[12] or others using biological components such as proteins or DNA to attach the AuNPs onto the CdSe QDs[13] to study their interactions.

Our group has previously reported the stabilization of CdSe QDs by Frechet-type carbazole dendrons both by direct synthesis [14] and ligand exchange methods.[15] Chalcogenide and semiconductor QDs are known for their wide absorbance spectra but narrow tunable fluorescence emission. When coupled with electroactive ligands, these QDs act as electron acceptors whereas the ligands act as donors. Electroactive surfactants such as the carbazole dendrons were found to facilitate electron transfer to the electron acceptor CdSe, hence making these hybrid nanoparticles suitable materials for photovoltaic and solar cells applications.[16] In another work, we have shown the *in situ* reduction of Au^{3+} to Au (0) by the carbazole end group attached to the amine groups of a G-4 polyamidoamine (PAMAM) dendrimer.[17] The synthesis of Au-NPs as DENs or

dendrimer encapsulated nanoparticles have been studied extensively by the Crook's group where they typically used the PAMAM as a template for the growth of small Au-NPs chemically reduced into the interior of the dendrimer. In one of their papers, they cited that formation of Au-NPs can also be observed outside the dendrimer when the peripheral hydroxyl group of the dendrimer prematurely reduces the Au^{3+} ions.[18] Typically they use an external reducing agent to accomplish the metallization.

In this present work, we have successfully demonstrated a three-component hybrid organic-inorganic nanoparticle composed of CdSe QD core, stabilized by an electroactive carbazole ligand using generations one (G1CBzPO-CdSe) and two (G2CBzPO-CdSe) with phosphonic acid focal point. The synthetic process utilizes a direct synthesis method of encapsulating the CdSe quantum dots and a one-pot synthesis for AuNPs and clusters that are reduced from Au^{3+} to Au^{0} *in situ* by the peripheral carbazole units. In this case, no external reducing agent was used but instead the oxidation of the carbazole unit resulted in the reduction of Au^{3+} ions to Au^{0}. The distance between the fluorophoric QD and the peripheral carbazole units is theoretically at 1.6 nm, the length of one carbazole dendron (calculated, Spartan software) from the phosphonic acid focal group to the carbazole unit. The Au nanoclusters presumably form proximal to the terminal carbazole units. The system described herein is a direct synthesis method where the reduction of Au^{3+} to Au(0), simultaneously caused the cross-linking of the carbazole units enabling a three-component hybrid nanoparticle (GnCBzPO-CdSe-AuNP) system where n represents the generation of the ligand.

3.2. Experimental Section

3.2.1. Materials

All chemicals were purchased from Alfa Aesar and were used directly without further purification. Tetrahydrofuran (THF) was freshly distilled over sodium and benzophenone before use. All solvents were aspirated with nitrogen gas before use.

3.3.2. Characterization

^{1}H NMR spectra were recorded using JEOL ECS 400 spectrometer (400MHz). UV-Vis was recorded using Agilent 8453 Spectrometer. Fluorescence spectra were obtained using Perkin-Elmer LS45 luminescence spectrometer. Fluorescence lifetime decay was measured using PTI QuantaMaster(tm) Model QM-4 scanning spectrofluorometer with LaserStrobe utilizing 337.1 nm line N2 laser pump. Fluorescence lifetime data was processed using 1 to 4 Exponential Analysis. X-ray Photoelectron Spectroscopy (XPS) was done using a PHI 5700 X-ray photoelectron spectrometer equipped with a monochromatic Al Kr X-ray source (hν = 1486.7 eV) incident at 90^{0}, relative to the axis of a hemispherical energy analyzer. The spectrometer was operated both at high and low resolutions with pass energies of 23.5 and 187.85 eV, respectively, a photoelectron take off angle of 45^{o} from the surface, and an analyzer spot diameter of 1.1 mm. All spectra were collected at room temperature with a base pressure of 1 X 10^{-8} Torr. The peaks were analyzed first by background subtraction, using the Shirley routine.

All the samples were completely dried in argon gas prior to XPS measurements. Samples were prepared by spin casting onto plasma-cleaned silicon wafer substrate.

3.2.3. Synthesis

The synthesis of generation one carbazole dendron with the benzoate ester focal point (G1CBz $COOCH_3$) needed as starting material for this reaction has already been described in the previous chapter. The scheme for the synthesis of the generation one carbazole with phosponic acid (G1CBzPO) focal point is shown in Scheme 3.1.

The synthesis of the generation two carbazole dendrons follows the same method as the generation one carbazole dendrons in the following functionalization: reduction to alcohol, bromination, and phosphonate formation. The first step in synthesizing the second generation starts from a generation one carbazole with an –OH moiety and coupling this with a commercially available 3,5-dihydroxy-methyl benzoate through a Mitsunobu etherification reaction to form the generation two ester (G2CBz $COOCH_3$).

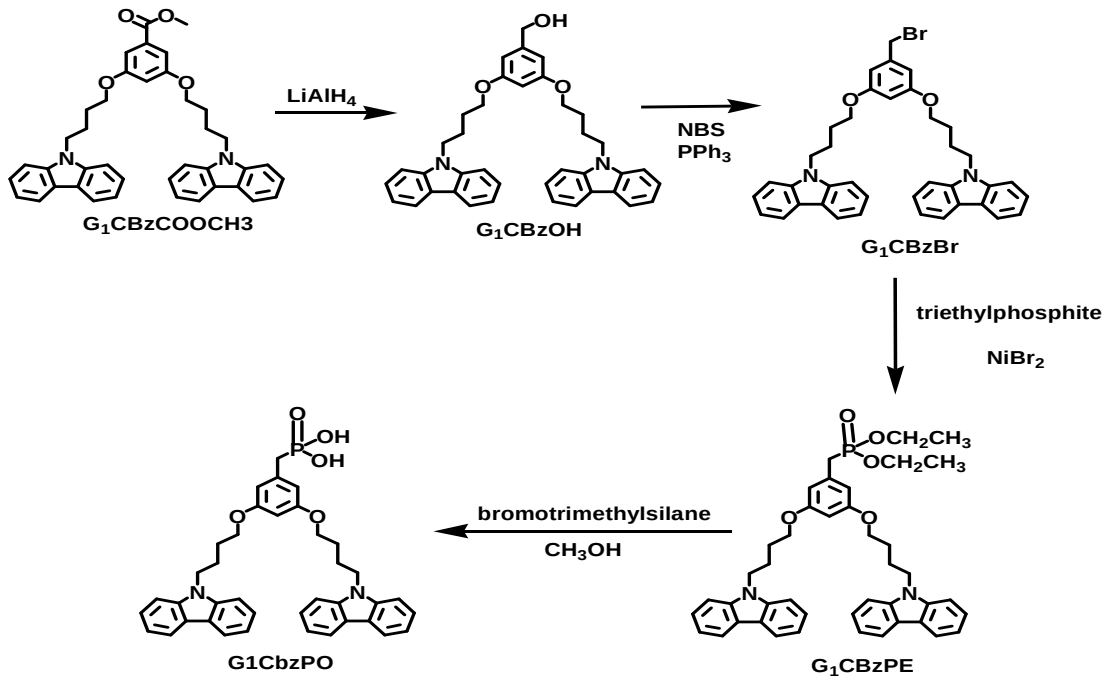

Scheme 3.1. Synthesis of G1CBzPO. Formation of the phosphonate follows an Arbuzov reaction with triethylphosphite attacking the halide in G_1CBzBr. Hydrolysis of the phosphonate affords the phosphonic acid functional group that anchors to the CdSe quantum dots.

Synthesis of 3,5-bis(4-(9H-carbazol-9-yl)butoxy)benzyl alcohol [G_1CbzOH]

The synthesis of compound G_1CbzOH was carried out by first dissolving G_1CbzCOOCH$_3$ (6.000 g, 9.80 mmol) in dry 70 mL THF. Into a 3-necked 250-mL round bottom flask flowed with nitrogen was placed 100 mL THF and this was cooled in an ice bath. Approximately 1.000 g $LiAlH_4$ was put into the flask and the G_1CbzCOOCH$_3$ solution was added dropwise through a dropping funnel. The resulting mixture was then stirred overnight. After which, the reaction was quenched by adding water until all the $LiAlH_4$ was consumed. This was then acidified with HCl and extracted with dichloromethane. The organic layer was further washed with water for several times and

then dried with Na_2SO_4. The dicholoromethane was evaporated using a rotary evaporator and the desired white solid powder was further dried under vacuum with a final yield of 93%. ^{1}H NMR (δ ppm in $CDCl_3$): 8.09 (d, *J* = 7.5 Hz, 4H), 7.47-7.18 (m, 12H), 6.43 (s, 2H), 6.27 (s, 1H), 4.57 (d, *J* = 5.7 Hz, 2H), 4.38 (t, *J* = 6.9 Hz, 4H), 3.90 (t, *J* = 5.9 Hz, 4H), 2.09-2.01 (m, 4H), 1.84-1.79 (m, 4H).

Synthesis of 3,5-bis(4-(9H-carbazol-9-yl)butoxy)benzyl Bromidel [G_1CbzBr]

Bromination of the generation one carbazole was achieved by substitution reaction where triphenyl phosphine was used as the base and N-bromosuccinimide (NBS) as the bromination reagent. Briefly, G1CBzOH (1.0 g, 1.7 mmol) and PPh_3 (0.675 g, 2.6 mmol) were dissolved in dry THF. This was purged in nitrogen at constant stirring. A solution of NBS/dry THF containing NBS (0.458 g, 2.6 mmol) was added dropwise using a syringe. This was allowed to stir for 3 hours until reaction was complete as checked on TLC plate using 4:1 CH_2Cl_2: hexane as eluent. Upon completion of the reaction, the solvent was dried in vacuo and extracted with CH_2Cl_2, washed with water, dried with Na2SO4. The CH_2Cl_2 was evaporated up to minimal amount and the product was purified on silica gel column using 3:2 CH_2Cl_2: hexane as solvent. Fine white powder wiyh 46 % yield was obtained as product. ^{1}H NMR (δ ppm in $CDCl_3$):8.10 (d, *J* = 7.8 Hz, 4H), 7.46-7.41 (m, 8H), 7.26-7.20 (m, 4H), 6.46 (d, *J* = 1.8 Hz, 2H), 6.28 (t, *J* = 2.3 Hz, 1H), 4.39 (t, *J* = 6.88 Hz, 4 H), 4.36 (s, 2H), 3.89 (t, *J* = 6.2 Hz, 4H), 2.09-2.03 (m, 4H), 1.85-1.80 (m, 4H), 1.56 (s, 4H).

Synthesis of 3,5-bis(4-(9H-carbazol-9-yl)butoxy)benzyl phosphonate Ester [G_1CbzPE]

The synthesis of the G1CBz-phosphonate ester followed the Michaelis-Arbuzov reaction. G1CBz-Br (1.070 g, 1.70 mmol) and $NiBr_2$ (0.413 g, 1.90 mmol) were placed in a Schlenck flask. This was stirred in nitrogen, after which 0.80 mL of triethylphosphite was slowly added using a syringe. This was freeze-thawed in vacuum three times and was heated in an oil bath to 135 ˚C. After 4.5 hours, the solution turned into a yellow sticky oil. This was cooled to room temperature and dissolved in minimal CH_2Cl_2 and was vacuum distilled using head distillation set-up to remove excess triethylphosphite. This was redissolved in CH_2Cl_2 and purified through silica gel with 3% MeOH/CH_2Cl_2 as eluent. Final product appears as yellowish oil with a yield of 60%. ^{1}H NMR (δ ppm in $CDCl_3$): 8.16 (d, *J* = 7.8 Hz, 4H), 7.52-7.49 (m, 4H), 7.46-7.43 (m, 4H), 6.49 (t, *J* = 2.3 Hz, 2H), 6.33 (d, *J* = 1.8 Hz, 1H), 4.37 (t, *J* = 6.86 Hz, 4H), 4.10 - 4.06 (m, 4H), 3.92(t, *J* = 5.96 Hz, 4H), 2.11- 2.05 (m, 4H), 1.88-1.82 (m, 4H), 1.30 (t, *J* = 7.3 Hz, 6H).

Synthesis of 3,5-bis(4-(9H-carbazol-9-yl)butoxy)benzyl Phosphonic acid [G_1CbzPO]

G1CBzPE was subsequently reacted to produce G1CBz-phosponic acid (G1CBzPO). G1CBzPE (1.700 g, 2.400 mmol) was dissolved in CH_2Cl_2 to which bromotrimethylsilane (1.110 g, 6.500 mmol) was added under nitrogen. This was stirred in ice bath for 2 hours and was evaporated to dryness to remove excess silane. This was redissolved in methanol and was refluxed for 4 hours. This was purified on silica gel with

10% MeOH:CH_2Cl_2. Purified product appeared as off-white crystals with 30 % yield. ^{1}H NMR (δ ppm in DMSO-d6): 8.08-8.04 (m, 4H), 7.52-7.47 (m, 4H), 7.36-7.32 (m, 4H), 7.13-7.08 (m, 4H), 6.34-6.29 (d, *J*= 20 Hz, 2H), 6.09-6.07 (d, *J*= 8 Hz, 1H), 4.38-4.29 (m, 4H), 3.75-3.5 (m, 6H), 1.8-1.7 (m, 4H), 1.6-1.5 (m, 4H), 1.19 (s, 1H), 0.86-0.84 (m, 3H).

Synthesis of methyl 3,5-bis(3',5'-bis(4-(9H-carbazol-9-yl)butoxy)benzyloxy) benzoate [G_2CBzCOOCH$_3$]

Synthesis of the generation two dendrons starts with a Mitsunobu etherification reaction of the G1CBzOH. Briefly, a pre-cooled solution of methyl 3,5-dihydroxybenzoate (0.860 g, 5.15 mmol), G1CBzOH (6.00 g, 10.3 mmol), and PPh_3 (2.70 g, 10.3 mmol) in THF under sonication was treated with a solution of DIAD (2.08 g, 10.3 mmol) in 3 mL THF under nitrogen. The solution was sonicated for 1.5 hours to afford a white solid product in 84% yield after purification. ^{1}H NMR (δ ppm in $CDCl_3$): 8.09 (d, *J* = 7.5 Hz, 8H), 7.48-7.39 (m, 16H), 7.27-7.21 (m, 8H), 7.19(d, *J* = 2.1 Hz, 2H), 6.76 (t, *J* = 2.1 Hz, 1H), 6.50 (d, *J* = 2.1 Hz, 4H), 6.31 (t, *J* = 2.1 Hz, 2H), 4.94 (s, 4H), 4.37 (t, *J* = 7.5 Hz, 8H), 3.91-3.87 (m, 11H), 2.08-2.03 (m, 8H), 1.85-1.78 (m,8H).

Synthesis of (3,5-bis(3',5'-bis(4-(9H-carbazol-9-yl)butoxy)benzyloxy)phenyl) methanol [G_2CBzOH]

Following the general synthesis of G1CBzOH as described above, the reaction of LAH (0.200g, 5.50 mmol) in 100 mL of THF with a solution G2CBzCOOCH$_3$ (4.2 0 g,

3.20 mmol) in 25 mL dry THF afforded a white solid product in 90% yield. ^{1}H NMR (δ ppm in $CDCl_3$): 8.15 (d, *J* = 7.5 Hz, 8H), 7.53-7.42 (m, 16H), 7.31-7.25 (m, 8H), 6.59 (d, *J* = 2.1 Hz, 2H), 6.50-6.52 (m, 5H), 6.32 (t, *J* = 2.1 Hz), 4.95 (s, 4H), 4.59 (s, 2H), 4.36 (t, *J* = 6.9 Hz, 8H), 3.88 (t, *J* = 5.7 Hz, 8H), 2.11-2.00 (m, 8H), 1.87-1.76 (m, 8H).

The synthesis of the G2CBzBr to G2CBzPO follows the same protocol as described in the synthesis of the generation one dendrons with these focal points. This is schematically described in Scheme 3.2.

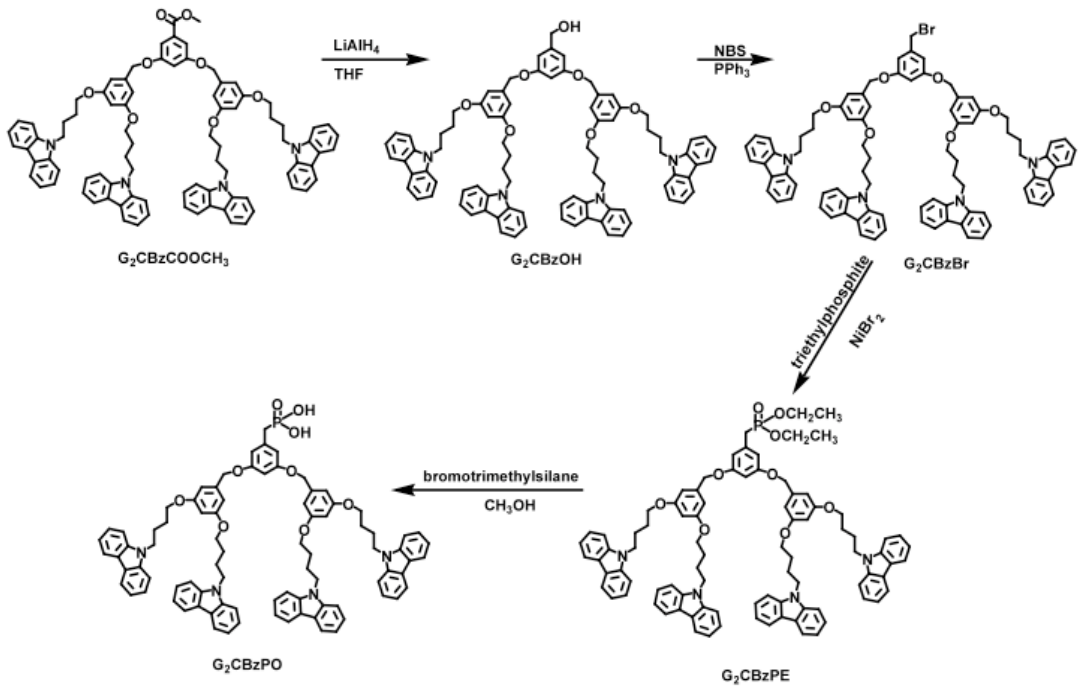

Scheme 3.2. Synthesis of G_2CBzPO . Generation two dendrons starts with Mitsunobu etherification of the G1-CBzOH with methyl-3,5-dihydroxybenzoate to form G_2CBzCOOCH$_3$.

Synthesis of GnCBzPO-capped CdSe Quantum Dots (n=1 for G1 and 2 for G2)

The synthesis of carbazole-functionalized CdSe quantum dots adapted a procedure previously reported by our group.[14] The same procedure is followed for both generations one and two. G1CBzPO/G2CBzPO with mass 23.3 mg / 50.0 mg , 0.0362 mmol) was placed in a Schlenck flask and to this was added 2.24 mg (0.00970 mmol) of CdO powder, 300 mg of dodecylamine (1.09 mmol) , and 4.8 mg (0.0289 mmol) of hexylphosphonic acid. This was tightly capped and was purged with N_2 gas and was heated slowly under vacuum to about 120 ˚C with vigorous stirring until the mixture turned into a red solution. Afterwhich, the heat was increased to reach 220 ˚C. As soon as the reaction mixture turned yellow, 5.0 mL Se-TOP solution (250 mg of Se powder in 5.0 mL trioctyl phosphine), previously degassed with N_2, was rapidly injected into the mixture. The mixture slowly turned pale yellow and eventually turned deep red in less than 1 minute. As soon as the desired size of the quantum dots was achieved based on color change, the mixture was removed from heat and cooled to around 60 ˚C. A previously degassed chloroform solvent was added to the mixture. Purification of CdSe-G1CBzPO/G2CBzPO was done by mixing 1.0 mL of the mixture and 0.5 mL degassed MeOH in 1.5 mL-centrifuge tubes. These were centrifuged for 15 mins at 12.3 rpm. The top MeOH layer was removed and this cycle was repeated until no unbound reactants were detected in the MeOH layer by UV-vis spectroscopy. The purified CdSe-G1CBzPO/G2CBzPO sample was dried in vacuum and was redispersed in chloroform. The product gave a luminescent red orange chloroform solution.

Synthesis of CdSe-GnCBzPO-AuNP (n=1 for G1 and 2 for G2)

The reduction of gold ions from $HAuCl_4$ to Au(0) was achieved using the carbazole units in CdSe-GnPO as reducing agents. 2.0 mL of 1 mM of $HAuCl_4$ in MeOH was slowly added to 2.0 mL of the CdSe-GnPO solution described above. The flow rate of the gold solution was fixed at 1.0 mL per hour into a vigorously stirred solution. After addition of the $HAuCl_4$ solution, this was left stirring for 24 hours under nitrogen at room temperature. The solution turned from yellow to deep red solution indicating the formation of gold nanoparticles. The solution was purified by centrifugation as described above, using Milli-Q water for washing to ensure that the unreacted excess Au^{3+} ions are washed away by the water. Presence of Au^0 was characterized using X-ray photoelectron spectroscopy and UV-Vis absorbance spectroscopy.

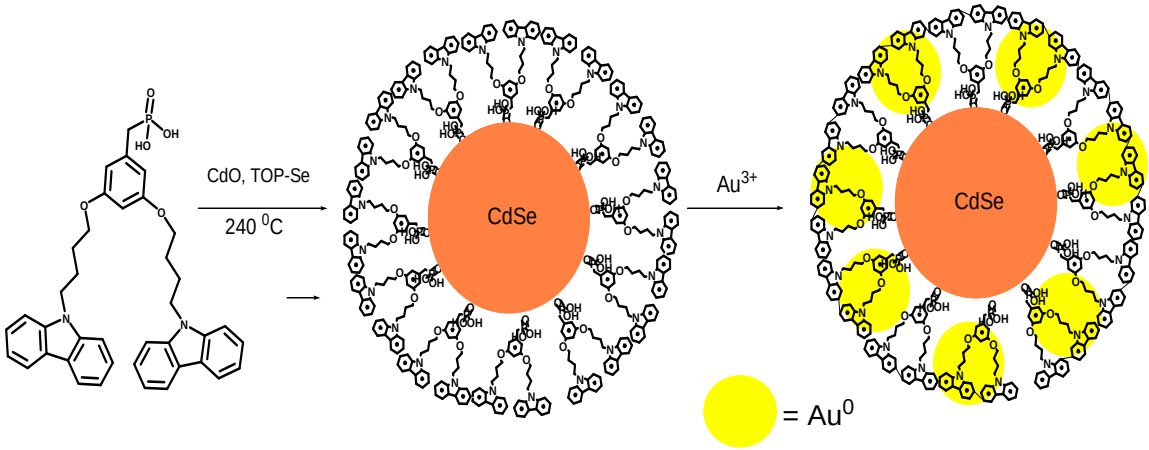

Scheme 3.3. Synthesis of G1- and G2CBzPO-Cdse-AuNP. Capping of CdSe with the dendrons is done in a one-pot synthesis. Formation of AuNPs from Au^{3+} resulted in simultaneous crosslinking of carbazole dendrons.

3.3. Results and Discussion

3.3.1.Absorption and Emission Properties

The synthesized hybrid nanoparticle was optically analyzed by UV-Vis absorption and fluorescence emission. Figure 3.1 depicts the absorbance of both generations of carbazole dendrons as capping agents for the as-synthesized CdSe quantum dots. The observed peaks at 326 nm and 346 nm correspond to the characteristic $\pi \rightarrow \pi^*$ and $n \rightarrow \pi^*$ transitions of the carbazole units, while the peaks at 470 nm and 560 nm are for the excitonic peaks of the CdSe quantum dots. The absorbance of the generation two dendrons shows a more pronounced carbazole intensity also at 333 nm and 346 nm due to greater number of carbazole and still showed peaks at 468 nm and 561 nm for the CdSe absorbance. Since the formation of the CdSe and the AuNP are both done as a one -pot direct synthesis, the absorbance of the AuNP in citrate and that of the CdSe-TOPO are also shown in Figure 3.1c and d respectively to serve as control variables from which to compare the similarity of the absorbance of the as synthesized nanoparticles. The AuNPs in citrate shows a plasmonic band at 520 nm and the CdSe-TOPO at 517 nm.

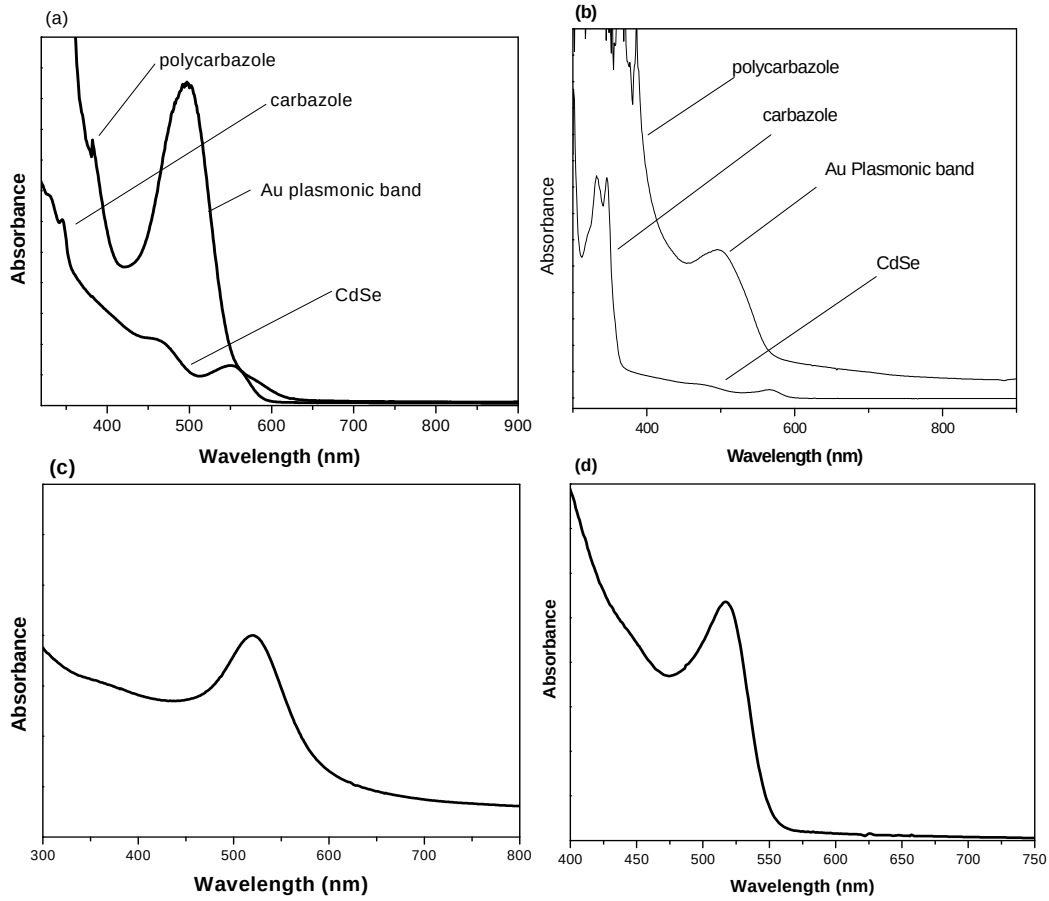

Figure 3.1. UV-Vis spectra of (a) G1- and (b) G2-CBzPO-Cdse with and without AuNP, (c) AuNP in citrate and (d) CdSe-TOPO. Formation of AuNPs is indicated by the broad plasmonic band around 500 nm that masks the absorbance of the CdSe. Red shifting of the carbazole peaks indicates chemical crosslinking of the dendrons..

Stirring $HAuCl_4$ into the carbazole-capped QDs resulted to the *in situ* oxidation of the carbazole dendrons as depicted by a significant red shift to around 400 nm suggesting the formation of cross-linked polycarbazole in Figure 3.1 (a) and (b). The generation two carbazole likewise showed a red shift from 347 nm to 386 nm upon cross-linking. The same absorbance peak shifting was seen in a previous paper where electrochemical

polymerization of the carbazole units formed polycarbazole around CdSe QDs or as a cross-linked matrix by cyclic voltametry.[14] Upon the formation of AuNP around the CdSe QDs, a red shift of 43 nm in the absorption spectra of the carbazole dedron-CdSe suggests a simultaneous oxidation and cross-linking of the carbazole with the reduction of the Au^{3+} to Au^{0}. This peak shifting confirms the formation of a highly conjugated nature of the carbazole species present in the system.[14]

3.3.2. X-ray Photoelectron Spectroscopy

The formation of the AuNPs and nanoclusters is further evidenced by high resolution X-ray photoelectron spectra (XPS) shown in Figure 3.2 (a) and (b) where the binding energy peaks of Au (0) is centered at 84.8 eV and 88.5 eV corresponding to $4f^{5/2}$ and $4f^{7/2}$, respectively for the generation one dendrons and 86.21 eV and 89.91 eV for generation two, a binding energy difference of 3.67 eV. The XPS spectrum of Cd in the form of CdSe (Figure 3.2 c and d) signified that the structure of the QDs is left intact during the formation of the gold nanoparticles for both generations. The broad plasmonic band centered at 504 nm in Figure 3.1 (a) and (b) suggests a AuNP size of 2-3 nm.[19] Typically, AuNPs >2nm have absorbance peak ranging from 500-550 nm.[20] It is also possible to ascribe the formation of Au nanoclusters since this is intermediate to the formation of AuNPs, even in an Ostwald ripening process. Theoretically, the distance between the fluorophoric QD and the peripheral carbazole units is at 1.6 nm, the length of one carbazole dendron from the phosphonic acid focal group to the carbazole unit as

calculated by Spartan Software in their lowest energy state. The Au nanoparticles or nanoclusters presumably form proximal to the terminal carbazole units through the nitrogen site.[21]

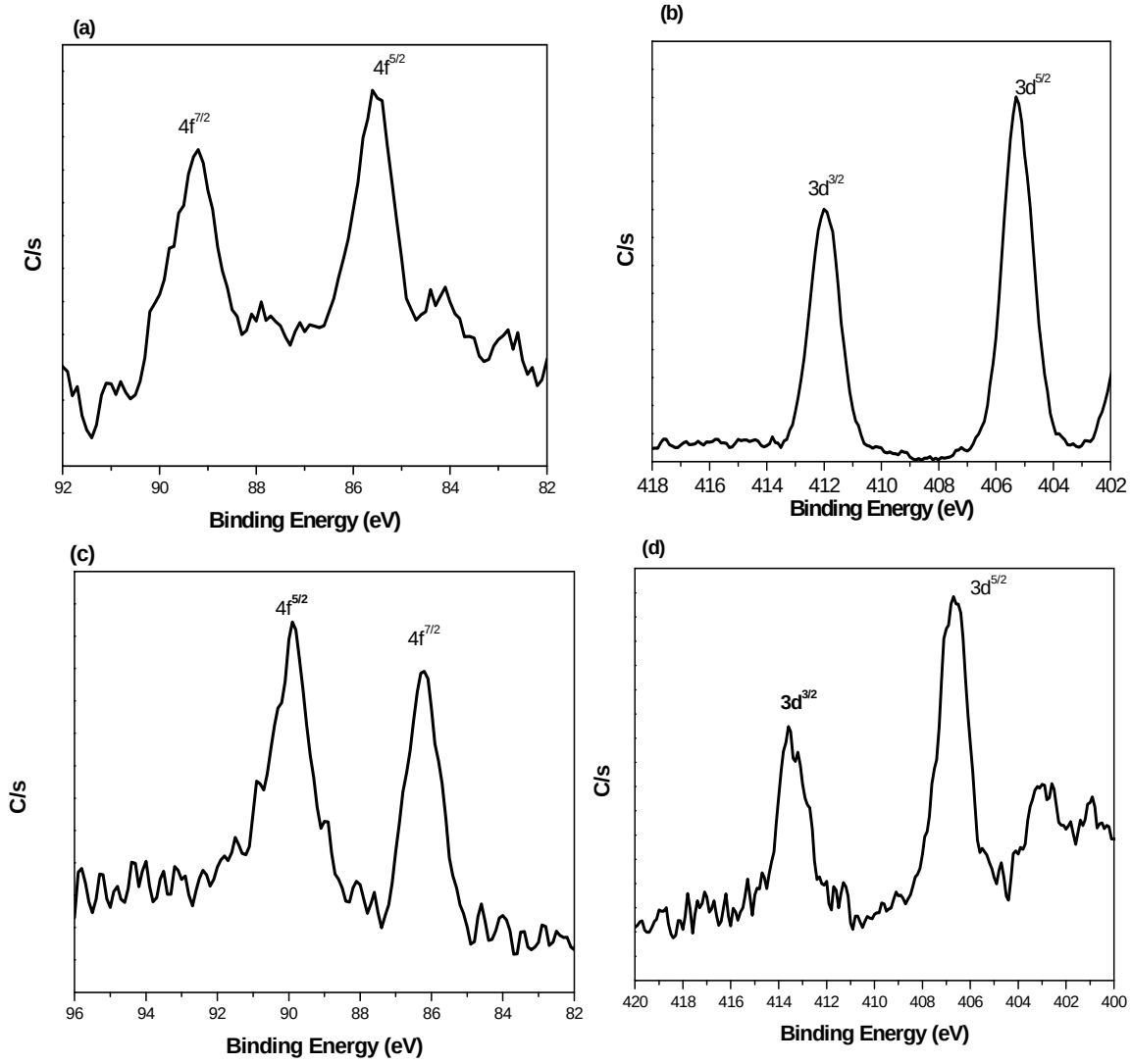

Figure 3.2. XPS spectra of G1- and G2CBzPO-CdSe-AuNP for Au(0) and Cd in the form of CdSe. Binding energies at 84.8 eV and 88.5 eV confirms formation of Au (0) with binding energy difference of 3.67 eV.

The XPS data confirmed the reduction of Au and the presence of some trace amounts of Au^{3+} that may not have completely reduced, observed at 90.2 eV and 86.6 eV.

3.3.3. Energy Transfer and Fluorescence Lifetime Decay

Energy transfer (ET) studies the optical properties of these materials wherein the ET is evidenced by either quenching of the emission of the donor and the consequent increase in emission of the acceptor or it can also be evidenced by the decrease in the excited state lifetime of the donor.[22] The efficiency of the energy transfer can also be determined by fluorescence lifetime based on the following equation:

$$E_t = 1 - {}^{\tau_{da}}/_{\tau_d}$$

where E_t is the energy transfer between the fluorophores and the acceptor, and $\boldsymbol{\tau}_{da}$ and $\boldsymbol{\tau}_d$ refer to the lifetime with and without the acceptor. Again, the efficiency is higher if the fluorescence lifetime of the donor is sufficiently decreased in the presence of the acceptor which acts as the quencher.

The occurrence of energy transfer in this system can be investigated by the change in the emission spectra of the dendron-capped CdSe QDs with and without the gold nanoparticles. In Figure 3.3 (a) and (b), it can be observed that the G1 carbazole showed emission at 350 and 375 nm when excited at 340 nm. For the generation two dendron with CdSe, the emission peak at 373 nm (without Au) shifted to 473 nm upon the formation of AuNP when excited at 340 nm. Since the QDs were synthesized directly

with the G1CBzPO and G2CBzPO shell-ligand, the emission of the CdSe QDs as a control was measured from a separately synthesized CdSe-TOPO whose emission peak is prominent at 549 nm (Figure 3.3 a) when excited at 400 nm. The electron transfer mechanism from the ligand to the QD core caused the emission intensity of the QD to decrease significantly.[14] For both sets of spectra, the presence of the AuNP (right) shows a much stronger quenching of the emission of the quantum dots that might be due to the proximal Au (0) acting as an energy acceptor.

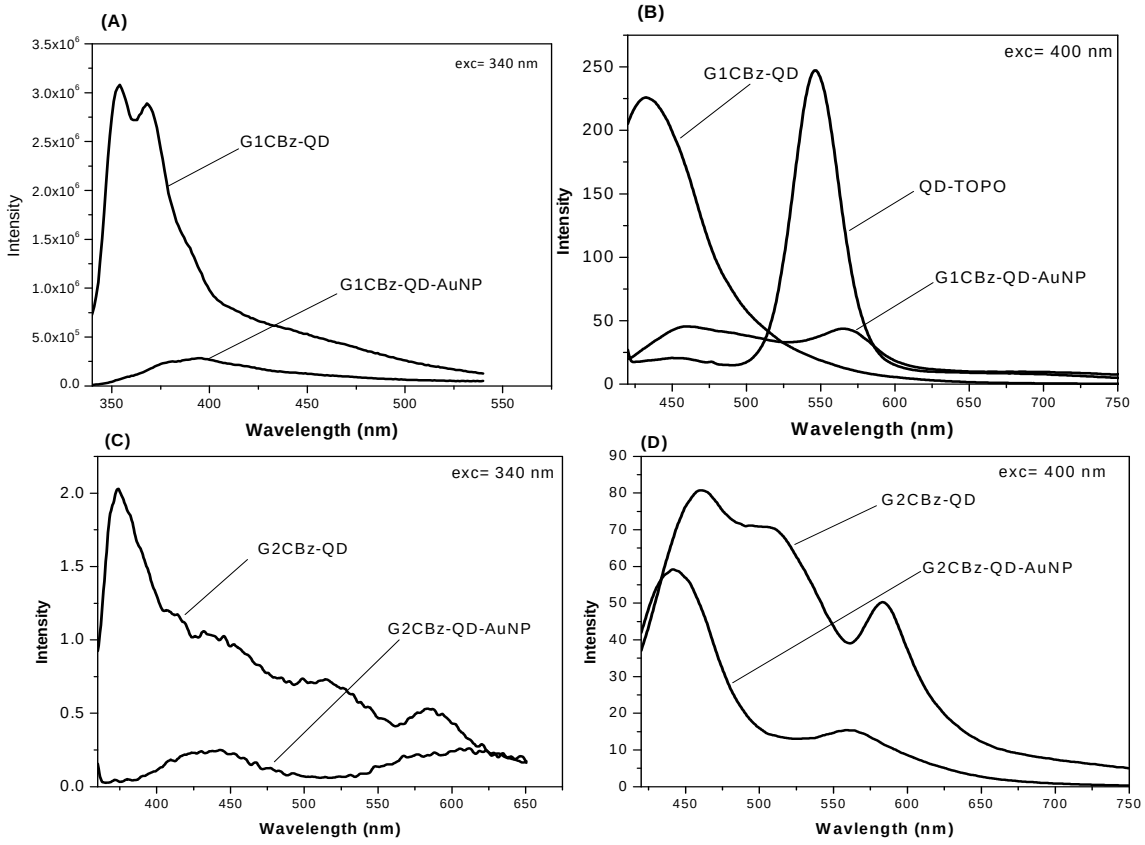

Figure 3.3. Emission spectra of (a) G1- and (b) G2CBz-QD with and without AuNP excited at 340 nm (left) and 400 nm (right). Samples were prepared in chloroform solution with the same concentration for with and without AuNPs.

The formation of AuNP in the vicinity of the CdSe core is evidenced by time-resolved fluorescence lifetime measurements. Table 1 summarizes the fluorescence lifetime decay of the CdSe-TOPO, G1CBzPO-QD, G1CBzPO-QD-AuNP, G2CzPO-QD, and G2CBzPO-QD-AuNP where a decreasing trend is observed. The lifetime of the CdSe in the absence (6.02 ns) and presence (1.92 ns for generation one) and (3.46 ns for generation two) of the carbazole ligands shows an increase in the decay rate that might be attributed to the electron transfer from the ligand to CdSe quantum dots.

The lifetime data further shows that the G1CBzPO-QD-AuNP and G2CBzPO-QD-AuNP has two molecular environments that contribute to a weighted average decay of 1.07 ns and 0.14 ns respectively as seen in Figure 3.4 and Table 3.1, in that 69.3 % of the hybrid nanoparticle contributes 0.74 ns and 30.7% contributes 1.8 ns with the latter showing more characteristic of the G1CBzPO-QD. The G2CBzPO-QD-AuNP shows two different molecular environment as well wherein 85.7% gives a lifetime of 0.072 ns and 14.3 % gives a lifetime contribution of 2.81 ns. This change in lifetime is further evidence of the presence of AuNPs and nanoclusters in the vicinity of the CdSe core but not exclusively on all the G1- and G2-CBzPO-QD. Comparing the efficiency of the energy transfer of the two nanocomposite based on fluorescence lifetime decay, the G2CbzPO-QD-AuNP showed a more efficient energy transfer averaging less than a nanosecond of decay.

The presence of the proximal AuNPs can efficiently account for the attenuated fluorescence of the QD core given the small distance between them. Several studies of

gold as a fluorescence quencher have been reported: whether they are too close or if they are directly paired or physically adsorbed with a donor organic fluorophore is a matter of synthetic approach or design.[23]

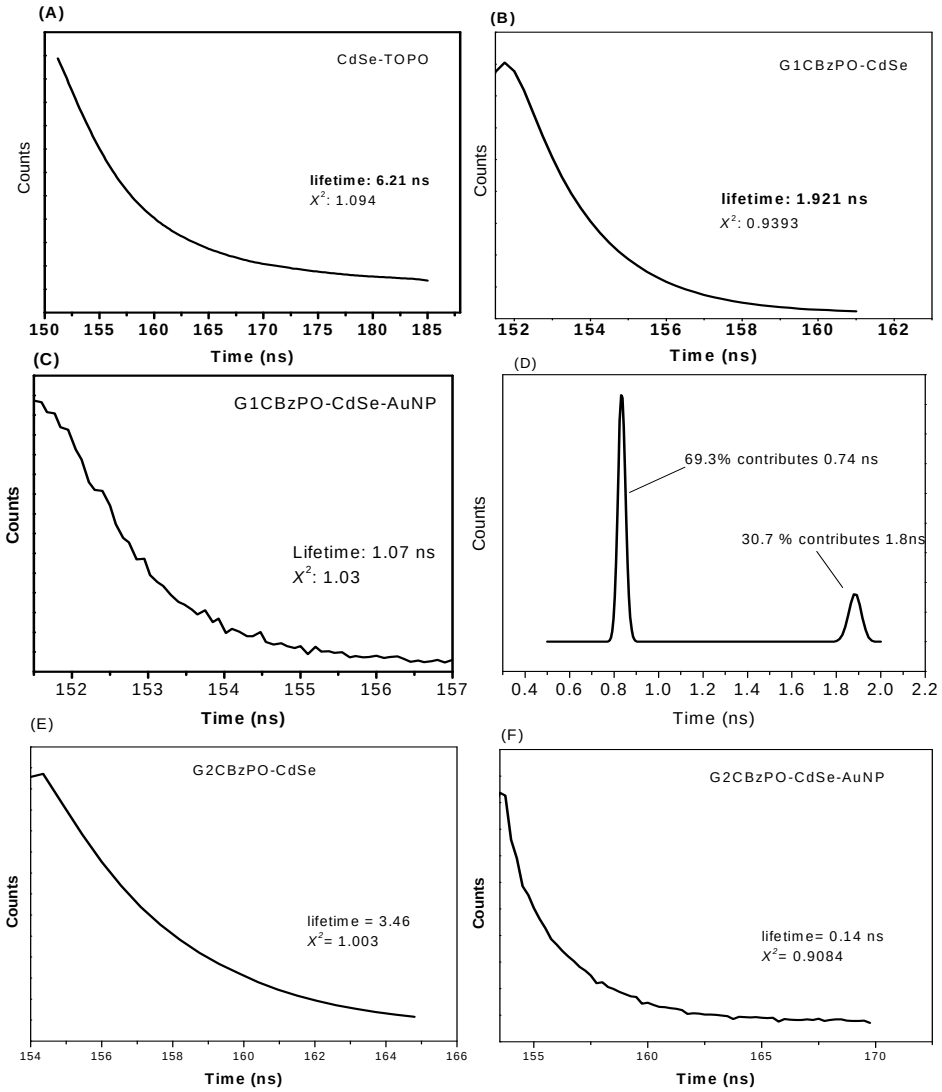

Figure 3.4. Fluorescence lifetime decay curves of (a) CdSe-TOPO, G1CBzPO (a) with and (c) without AuNP, (d) the lifetime distribution for G1CBzPO-CdSe-AuNP, (e) G2CBzPO-CdSe and (f) G2CBzPO-CdSe-AuNP. Decrease in fluorescence lifetime indicates ET between AuNPs and CdSe.

In this case, while not all G1- and G2CBzPO-QD may have participated in the reduction process, nor all AuNPs or clusters remained in the vicinity of the QDs, the "one pot" synthesis enables proximal spacing, enough to affect the steady state and time-resolved fluorescence of the hybrid QDs. We can attribute the quenching mechanism as a non-radiative energy transfer from the fluorescent quantum dots to the proximal gold nanoparticles since the emission of the QDs overlap with the absorbance of the Au nanoparticle. FRET or NSET mechanism can be further investigated to support this study.

Table 3.1. Average fluorescence lifetime data of CdSe-TOPO, G1- and G2-CBzPO-CdSe with and without the AuNP. Lifetime data is processed using 1 to 4 exponential analysis.

Sample	**Molecular Fraction**	**τ^a[ns]**	**$\langle\tau\rangle^b$[ns]**	**$\chi^{2\,c}$**
CdSe-TOPO	1	6.02	6.02	1.094
G1CBzPO-CdSe	1	1.92	1.92	0.939
G1CBzPO-CdSe-AuNP	0.693 0.307	0.74 1.80	1.07	1.030
G2CBzPO-CdSe	1	3.46	3.46	1.003
G2CBzPO-CdSe-AuNP	0.857 0.143	0.072 2.81	0.14	0.9084

[a] (lifetime), [b](average lifetime), [c] (goodness of fit)

3.4. Conclusions

In summary, we have reported energy transfer properties on a three-component organic-inorganic hybrid nanostructured particle where the CdSe QD core is capped by G1 and G2 carbazole dendrons. This carbazole periphery enabled the formation of

plasmonic AuNPs and nanoclusters formed within the vicinity by reducing the Au^{3+} ions to Au^{0} without the use of external reducing agent. The formation of the AuNPs and nanoclusters resulted in a shift of the absorbance and emission peaks of the carbazole group. The carbazole ligands initially quenched the fluorescence of the CdSe QD core. Furthermore, the proximal AuNPs acted as fluorescence acceptor, further quenching the fluorescence of the QDs. The formation of the G1- and G2-CBzPO-QD was done in a direct synthesis route followed by the *in situ* reduction of the AuNPs which did not require any ligand exchange of any other stabilizer nor any external reducing agent. Synthesis of generation three carbazole dendrons and lengthening the distance between the CdSe QDs and the AuNPs by conjugating a spacer onto the ligand would be an interesting investigation to pursue to see the quenching or other energy transfer mechanisms involving distance dependence between a hybrid CdSe QDs and AuNP assembly.

3.5. References

1. (a) Standridge, S. D.; Schatz, G. C.; Hupp, J. *Langmuir* **2009**, *25*, 2596. (b) Bhandari, S.; Deepa, M.; Sharma, S.; Joshi, A. G.; Srivastava, A. K.; Kant, R. *J. Phys. Chem. C.* **2010**, *114*, 14606.
2. (a) Sheldon, M. T.; Trudeau, P. E.; Mokari, T.; Wang, L. W.; Alivisatos, A. P. *Nano Lett.* **2009**, *9*, 3676. (b) Guo, Z. S.; Zhao, L.; Pei, J.; Zhou, Z. L.; Gibson, G.; Brug, J.; Lam, S.; Mao, S. S. *Macromolecules* **2010**, *43*, 1860.
3. (a) Quach, A. D.; Crivat, G., Tarr, M. A.; Rosenweig, Z. *J. Am. Chem. Soc.* **2011**, *133*, 2028. (b) Tang, R.; Lee, H.; Achilefu, S. *J. Am. Chem. Soc.* **2012**, *134*, 4545. (c) Lowe, S. B.; Dick, J. A. G.; Cohen. B. E.; Stevens, M. M. *ACS Nano* **2012**, *6*, 851.
4. (a) Costi, R.; Saunders, A. E.; Elmalem, E.; Salant, A.; Banin, U., *Nano Lett.* **2008**, *8*, 637. (b) Subramanian, V.; Wolf, E. E.; Kamt, P. V. *J. Am. Chem. Soc.* **2004**, *126*, 4943. (c) Shemesh, Y.; MacDonald, J. E.; Menagen, G.; Banin, U. *Angew. Chem. Int. Ed.* **2011**, *50*, 1185.
5. (a) Barnes. W. L.; Derex, A.; Ebbesen, T. W. *Nature* **2003**, *424*, 824. (b) Eustis, S.; El-Sayed, M. A. *Chem. Soc. Rev.* **2006**, *35*, 209. (c) Daniel, M. C.; Astruc, D. *Chem. Rev.* **2004**, *104*, 291.
6. (a) Talapin, D. V.; Lee, J. S.; Kovalenko, M.; Shevchenko, E. *Chem. Rev.* **2010**, *110*, 389. (b) Burda, C.; Chen, X.; Narayanan, R.; El-Sayed, M. A. *Chem. Rev.* **2005**, *105*, 1025.

7. Huynh, W. U.; Dittmer, J. J.; Alavisatos, A. P. *Science* **2002**, *295*, 2425.

8. Shaviv, E.; Schubert, O.; Alves-Santos, M.; Goldoni, G.; Felice, R. D.; Vallee, F.; Del Fatti, N.; Banin, U.; Sonnichsen, C. *ACS Nano* **2011**, *5*, 4712.

9. (a) Gao, X.; Jin, Y. *Nature Nanotech.* **2009**, *4*, 571. (b) Pons, T., Medintz, I; Sapsford, K., Higashiya, S.; Grimes, A.; English, D.; Mattoussi, H. *Nano Lett.* **2007**, *7*, 3157. (c) Quach, A. D.; Crivat, G.; Tarr, M.; Rosenweig, Z. *J. Am. Chem. Soc.* **2011**, *133*, 2028.

10. (a) Bandari, S.; Deepa, M.; Sharma, S.N.; Joshi, A.G.; Srivastava, A.K.; Kant, R. *J. Phys .Chem. C* **2010**, *114*, 14606. (b) Bawendi, M. G.; Steigerwald, M. L.; Brus, L. E. *Annu. Rev. Phys.Chem* **1990**, *41*, 477. (c) Bardhan, R.; Grady, N.; Halas, N. *Small* **2008**, *4*, 1716. (d) Bardhan, R.; Grady, N.; Cole, J.; Joshi, A.; Halas, N. *ACS Nano* **2009**, *3*, 744.

11. (a) Figuerola, A.; van Huis, M.; Zanella, M.; Genovese, A.; Marras, S.; Falqui, A.; Zandbergen, H. W.; Cingolani, R.; Manna, L. *Nano Lett.* **2010**, *10*, 3028. (b) Menagen, G.; MacDonald, J. E.; Shemesh, Y.; Popov, I.; Banin, U. *J. Am. Chem. Soc.* **2009** *131*, 17406.

12. (a) Owen, J. S.; Chan, E. M.; Liu, H.; Alivisatos, A. P., *J. Am. Chem. Soc.* **2010,** *132*, 51. (b) Daou, T. J.; Li, Liang,; Reiss, P.; Josserand, V.; Texier, I., *Langmuir* **2009**, *25*, 3040.

13. (a) Oh, E.; Hong, M. Y.; lee, D.; Nam, S. H.; Yoon, H. C.; Kim, H.-S. *J. Am. Chem. Soc*. **2005**, *127*, 3270. (b) Li, M.; Cushing, S. K.; Wang, Q.; Shi, X.; Homak, L. A.; Hong, Z. Wu, N. *J. Phys. Chem. Lett.* **2011**, *2*, 2125.

14. Park, Y.; Taranekar, P.; Park, J. Y.; Baba, A.; Fulghum, T.; Ponnapati, R.; Advincula, R. C. *Adv. Func. Mater.* **2008**, *18*, 2071.

15. Locklin, J.; Patton, S.; Deng, S.; Baba, A.; Millan, M.; Advincula, R. C. *Chem. Mater*. **2004**, *16*, 5187.

16. (a) Milliron, D.; Alivisatos, A. P.; Pitois, C.; Edder, C.; Frechet, M. J. *Adv. Mater*. **2003**, *15*, 58. (b) Kongkanand, A.; Tvrdy, K.; Takechi, K.; Kuno, M.; Kamat, P. *J. Am. Chem. Soc.* **2008**, *130*, 4008.

17. Kaewtong, C.; Guoqian, J.; Ponnapati, R.; Pulpoka, B.; Advincula, R. C. *Soft Matter* **2010**, *6*, 5316.

18. (a) Gomez, M. V.; Guerra, J.; Velders, A. H.; Crooks, R. M. *J. Am. Chem. Soc.* **2009**, *131*, 341. (b) Scott, R. W. J.; Wilson, O. M.; Crooks, R. M. *J. Phys. Chem. B* **2005**, *109*, 692. (c) Knecht, M. R.; Garcia-Martinez, J. C.; Crooks, R. M. *Langmuir* **2005**, *21*, 11981. (d) Kim, Y. G.; Oh, S. K.; Crooks, R. M. *Chem. Mater*. **2004**, *16*, 167.

19. Brown, P.; Kamat, P. *J. Am. Chem. Soc*. **2008**, *130*, 8890.

20. Kim, Y.; Oh, S.; Crooks, R. M. *Chem. Mater.* **2004**, *16*, 167.

21. Gupta, B.; Joshi, L.; Prakash, R. *Macromol. Chem. Phys.* **2011**, *212*, 1692.

22. Berezin, M.; Achilefu, S. *Chem. Rev.* **2010**, *110*, 2641.

23. (a) Bardhan, R.; Grady, N.; Halas, N. *Small* **2008**, *4*, 1716. (b) Bardhan, R.; Grady, N.; Cole, J.; Joshi, A.; Halas, N. *ACS Nano* **2009**, *3*, 744.

Chapter 4. Conclusion and Future Work

4.1. Conclusions

This thesis has demonstrated facile one-pot synthesis methods of hybrid organic-inorganic nanoparticles using electroactive dendrons as stabilizing agents and reactor hosts. The energy transfer properties in the presence of gold nanoparticles combined with the optical properties of the dendrons resulted in quenching of the carbazole emission . On the other hand, emission shifts with the CdSe quantum dot core and Au-nanoclusters in the periphery were established using steady state and time resolved fluorescence spectroscopy. These have been the important findings of this study with a high potential for optoelectronic and solid-state devices, in particular:

In Chapter 1, an overview of the different structures, synthesis, characterization, and application of hybrid nanoparticles is presented. Various electroactive dendrons and polymers are described as well as the individual properties of previously reported hybrid gold nanoparticles (AuNPs) and CdSe quantum dots (QDs) with emphasis on the energy transfer involved when these components are proximal to each other.

Chapter 2 reported on the facile synthesis of a nanoparticle-cored dendrimer where a generation three PAMAM dendrimer with cystamine core and amine surface is functionalized with generation one carbazole dendron. This functionalization was done by amidation of the carboxylic acid focal point of the carbazole dendron with the amine surface of the PAMAM dendrimer. This was characterized by IR and UV-vis spectra.

The disulfide bond of the cystamine core is reduced forming a dendron wedge that stabilized the gold nanoparticles. Formation of gold nanoparticles was characterized by X-ray photoemission spectroscopy (XPS) and transmission electron microscope (TEM) where the size of the nanoparticle averaged at 4.1 nm. Energy transfer from this construct was investigated by decrease fluorescence lifetime decay and shifting in absorbance and emission peaks.

In Chapter 3, a three-component hybrid organic-inorganic nanoparticle was synthesized wherein CdSe quantum dots were formed in a one-pot synthesis with generations one (G1) and two (G2) carbazole with phosphonic acid focal point as capping agents. Gold nanoparticles were formed when gold ions where gradually added and were reduced by the simultaneous oxidation and cross-linking of the peripheral carbazole dendrons. The formation of the gold nanoparticles was characterized by XPS and optical properties. A surface plasmon resonance band was observed at 504 nm UV-Vis absorbance spectra. A red shifting of the absorbance and emission of the carbazole was also observed suggesting cross-linking of the carbazole thereby increasing its conjugation. Energy transfer is further investigated by the quenching of the emission of CdSe quantum dots by the presence of the proximal gold nanoparticles (AuNPs) as well as a decrease in the fluorescence lifetime. The G2-carbazole showed a higher efficiency of the energy transfer as the lifetime of this nanostructure showed greater decrease in fluorescence lifetime.

4.2. Future Work

There are several areas that can be added for future work: 1) Quantitative investigation on the percent conjugation of carbazole dendrons on the G3PAMAM dendrimer can be investigated to optimize the synthetic protocol and determine the quenching effect by steady state emission using equal concentrations of the dendrimer with and without AuNPs. 2) Optical properties after electropolymerization can also be added to study its viability for optoelectronic applications in solid-state devices and for further investigation of the energy or charge transfer mechanism involved upon excitation from surfaces, e.g. evanescent waveguides and electrodes. 3) Further proof of structure can be determined by high resolution TEM to visually investigate the position of the nanoparticles with respect to the dendrimers and its histogram. In addition, optimizing the ratio of the concentration of the Au^{3+} to the concentration of the dendrimers can also be studied to produce a more monodispersed size of the gold nanoparticles produced. 4) Lastly, it is the intention in this project to incorporate CdSe quantum dots at the periphery of the dendrimer to investigate FRET or NSET mechanisms involved and study its possible application in photovoltaics or solar cell fabrication. A synthetic design to incorporate these quantum dots in the carbazole units will be a promising project.

Manipulating the distance between the gold nanoparticles and the CdSe quantum dots by lengthening the chain of the focal point of the dendron can be included in the future work to investigate FRET mechanism involved between donor CdSe and acceptor

AuNPs. Higher generation of the dendrons can also be synthesized to provide a greater void space to house gold nanoparticles. Optimizing the ratio between the gold ions and the CdSe-carbazole can improve the monodispersity of the size of the AuNP produced. High resolution transmission electron microscopy (HR-TEM) can also be utilized to have a better visual inspection of the synthesized nanostructure. More quantitative energy transfer investigation can also be done for optimization of synthetic design and thin film fabrication.

4.3 Final Remarks

The energy transfer involved between gold nanoparticles and quantum dots is a highly investigated field for a wide variety of applications involving optoelectronic devices such as LEDs, photovoltaic cells, organic solar cells, as well as for bio-imaging and sensors. This thesis has demonstrated facile one-pot synthesis methods of these hybrid nanostructures and incorporated organic materials into inorganic crystals for easier fabrication of these devices with efficient charge transfer or energy transfer phenomenon. These materials should be suited for electrochemical deposition of ultrathin films having carbazole peripheral groups. Controlling the size of the nanoparticles and the distance of the components with respect to each other are defining parameters for future synthetic efforts.